MUTANT PrP IS DELAYED IN ITS EXIT FROM THE ENDOPLASMIC RETICULUM, BUT NEITHER WILD-TYPE NOR MUTANT PrP UNDERGOES RETROTRANSLOCATION PRIOR TO PROTEASOMAL DEGRADATION*

Bettina Drisaldi[‡§¶], Richard S. Stewart[‡¶], Cheryl Adles[‡], Leanne R. Stewart[‡], Elena Quaglio[‡‖], Emiliano Biasini[‖], Luana Fioriti[‖], Roberto Chiesa[‖], and David A. Harris[‡ ‡‡]**

[‡]Department of Cell Biology and Physiology
Washington University School of Medicine
St. Louis, MO 63110 USA

[‖]Dulbecco Telethon Institute (DTI) and Department of Neuroscience, Istituto di Ricerche Farmacologiche "Mario Negri", Milano 20157, Italy

Downloaded from http://www.jbc.org/ by guest on March 24, 2020

*This work was supported by a grant to D.A.H. from the NIH (NS35496); and to R.C. from Telethon-Italy (TCP00083) and the EC (QLG-CT-2001-2353). R.C. is an Assistant Telethon Scientist (DTI, Fondazione Telethon).

[§]Current address: University of Toronto, Center for Research in Neurodegenerative Diseases, Tanz Neuroscience Bldg., 6 Queen's Park Crescent West, Toronto, Ontario M5S 3H2 Canada.

[¶]These two authors contributed equally to this work.

[**]Current address: Istituto di Ricerche Farmacologiche "Mario Negri", Via Eritrea 62, 20157 Milano, Italy.

[‡‡]To whom correspondence should be addressed: Dept. of Cell Biology and Physiology, Washington University School of Medicine, 660 So. Euclid Ave., St. Louis, MO 63110, USA. Tel: 314-362-4690. Fax: 314-747-0940. E-mail: dharris@cellbio.wustl.edu.

[1]The abbreviations used are: CHO, Chinese hamster ovary; endo H, endoglycosidase H; ER, endoplasmic reticulum; GPI, glycosyl-phosphatidylinositol; PBS, phosphate-buffered saline; PDI, protein disulfide isomerase; PIPLC, phosphatidylinositol-specific phospholipase C; PrP, prion protein; PrP^{C}, cellular isoform of PrP; PrP^{Sc}, scrapie isoform of PrP; PSI 1, proteasome inhibitor 1 (Z-Ile-Glu(OtBu)-Ala-Leu-al); RT-PCR, reverse transcriptase polymerase chain reaction; SP, signal peptide; WT, wild-type.

Running Title: Biosynthesis and proteasomal degradation of PrP

SUMMARY

The cellular mechanisms by which prions cause neurological dysfunction are poorly understood. In order to address this issue, we have been using cultured cells to analyze the localization, biosynthesis, and metabolism of PrP molecules carrying mutations associated with familial prion diseases. We report here that mutant PrP molecules are delayed in their maturation to an endoglycosidase H-resistant form after biosynthetic labeling, suggesting that they are impaired in their exit from the endoplasmic reticulum (ER). However, we find that proteasome inhibitors have no effect on the maturation or turnover of either mutant or wild-type PrP molecules. Thus, in contrast to recent studies from other laboratories, our work indicates that PrP is not subject to retrotranslocation from the ER into the cytoplasm prior to degradation by the proteasome. We find that, in transfected cells but not in cultured neurons, proteasome inhibitors cause accumulation of an unglycosylated, signal peptide-bearing form of PrP on the cytoplasmic face of the ER membrane. Thus, under conditions of elevated expression, a small fraction of PrP chains is not translocated into the ER lumen during synthesis, and is rapidly degraded in the cytoplasm by the proteasome. Finally, we report a previously unappreciated artifact caused by treatment of cells with proteasome inhibitors: an increase in PrP mRNA level and synthetic rate when the protein is expressed from a vector containing a viral promoter. We suggest that this phenomenon may explain some of the dramatic effects of proteasome inhibitors observed in other studies. Our results clarify the role of the proteasome in the cell biology of PrP, and suggest reasonable hypotheses for the molecular pathology of inherited prion diseases.

Downloaded from http://www.jbc.org/ by guest on March 24, 2020

INTRODUCTION

Prion diseases, also called transmissible spongiform encephalopathies, are fatal neurodegenerative disorders that have attracted enormous scientific attention because they exemplify a novel mechanism of biological information transfer based on the transmission of protein conformation rather than on the inheritance of nucleic acid (1, 2). There is now considerable evidence that these diseases are caused by conformational conversion of PrP^{C} [1], a cell surface glycoprotein of uncertain function, into PrP^{Sc}, a β-rich and protease-resistant isoform that appears to be infectious in the absence of nucleic acid. This conversion can be catalyzed by exogenous PrP^{Sc} during infectious transmission, or can occur spontaneously in familial cases as a result of dominantly inherited, germline mutations in the PrP gene (3). Point mutations in the C-terminal half of the PrP molecule are associated with either Gerstmann-Sträussler syndrome, fatal familial insomnia, or familial forms of Creutzfeldt-Jakob disease. Insertional mutations, which produce a variable phenotype that can include features of both Creutzfeldt-Jakob disease and Gerstmann-Sträussler syndrome, consist of 1-9 additional copies of a peptide repeat that is normally present in 5 copies in the N-terminal half of the protein.

In order to understand how mutant PrP molecules cause neurological dysfunction in familial prion diseases, we have been analyzing the biochemical properties, metabolism and cellular localization of these proteins in cultured cells. We and others have found that mutant PrPs expressed in several different cell types acquire biochemical properties that are reminiscent of PrP^{Sc} (4-10). These properties include partial resistance to protease digestion, insolubility in non-denaturing detergents, and

Downloaded from http://www.jbc.org/ by guest on March 24, 2020

resistance of the C-terminal glycolipid anchor to cleavage by phospholipase. Although the protease resistance of the mutant PrPs synthesized in cultured cells is quantitatively less than that of many strains of PrP^{Sc} from infected brain, it is likely that the cultured cells are reproducing key steps in the metabolism of mutant proteins that are relevant to the pathogenesis of familial prion diseases. Indeed, transgenic mice expressing a similar, weakly protease resistant form of mutant PrP in their brains develop a fatal neurological illness with many similarities to human familial prion disorders (11, 12).

Several key results from our laboratory have identified the endoplasmic reticulum (ER) as a critical cellular compartment in the metabolism of mutant PrP molecules. First, pulse-chase labeling experiments indicate that PrP molecules carrying pathogenic mutations first become phospholipase resistant early in the secretory pathway, probably as a result of misfolding of the polypeptide chains during their synthesis in the ER (13, 14). Second, subcellular localization studies indicate that these same mutant PrP molecules accumulate in the ER and are expressed at reduced levels on the cell surface (15). Third, a mutant form of PrP, L9R/3AV, that is synthesized exclusively with a transmembrane topology is retained completely in the ER of cultured cells and is not detectably transported to the cell surface (16).

Interest in the role of the ER in PrP metabolism has been heightened recently by reports that both wild-type and mutant PrP molecules are recognized by the ER quality control machinery (17-19). It is well known that some membrane and secretory proteins, including several that are mutated in inherited human diseases, are recognized as abnormal soon after their synthesis as a result of misfolding of the polypeptide chain in the ER (20-22). These proteins are then transported backwards

Downloaded from http://www.jbc.org/ by guest on March 24, 2020

(retrotranslocated) through the translocon channel of the ER membrane into the cytoplasm, where they are degraded by the proteasome, often following conjugation to ubiquitin. The primary evidence for involvement of this pathway in the metabolism of PrP is the observation that treatment of cultured cells with proteasome inhibitors causes accumulation of an aggregated, unglycosylated form of PrP in the cytoplasm (17-19). It has also been reported that the cytosolic PrP found in inhibitor-treated cells displays properties of PrP^{Sc}, including protease resistance and the ability to sustain conversion of newly synthesized PrP^{C} to a PrP^{Sc} form (18). Finally, artificial expression of PrP in the cytoplasm using a PrP construct lacking the N-terminal signal sequence was found to be toxic to cultured cells, and resulted in a neurodegenerative phenotype in transgenic mice (23). On the basis of these results, the hypothesis has been advanced that mislocalization of PrP in the cytoplasm may be a general mechanism underlying the spontaneous formation of infectious PrP^{Sc}, as well as the pathogenesis of prion diseases (23). In addition, it has been cautioned that the therapeutic use of proteasome inhibitors in clinical settings may increase the risk for development of prion disease (23).

In the present paper, we have undertaken a detailed analysis of the metabolism of wild-type and mutant PrP molecules in cultured cells, and the effect of proteasome inhibitors on the turnover of these proteins. We find that mutant PrP molecules are delayed in their biosynthetic maturation, and exit the ER more slowly than wild-type molecules. In contrast to recent reports, however, we find that neither wild-type nor mutant PrP proteins are major substrates for retrotranslocation and proteasomal degradation. We observe that a small percentage of PrP chains is inefficiently translocated when the protein is expressed at high levels in transfected cells, and these

Downloaded from http://www.jbc.org/ by guest on March 24, 2020

chains are degraded by the proteasome without entering the ER lumen. We also suggest that some of the dramatic effects of proteasome inhibitors observed in previous studies are due to artifactual increases in PrP mRNA levels and protein synthetic rate, rather than to reduction in the catalytic activity of the proteasome. The work presented here clarifies an important current issue in the cell biology of PrP, and suggests reasonable hypotheses for the molecular pathology of prion diseases.

EXPERIMENTAL PROCEDURES

Cells. All expression constructs used in this paper carried a CMV promoter to drive synthesis of PrP in transfected cells. Stably transfected lines of CHO and PC12 cells expressing WT, PG14, or D177N-Met128 murine PrP from a pBC12 vector have been described previously (4, 5, 7, 24). The WT and PG14 proteins in these lines carried an epitope tag for the antibody 3F4. Plasmids containing the coding sequences for murine WT, PG14, or D177N-Met128 PrP (all 3F4 epitope-tagged) in the vector pcDNA3 (Invitrogen Corp., Carlsbad, CA) were transiently transfected into CHO or BHK cells using Lipofectamine (Invitrogen) according to the manufacturer's directions. Cells were used 24 hr after transient transfection. CHO and BHK cells were maintained in α-MEM supplemented with 10% fetal calf serum, non-essential amino acids, and penicillin/streptomycin. PC12 cells were grown in Dulbecco's modified Eagle's medium supplemented with 10% horse serum, 5% fetal calf serum, and penicillin/streptomycin.

Cultures of granule cells were prepared from the cerebella of Tg(WT-E1), Tg(PG14-A2), or Tg(PG14-A3) mice (12) at postnatal day 3-6 according to the

Downloaded from http://www.jbc.org/ by guest on March 24, 2020

procedure of Miller and Johnson (25). Briefly, cerebella were dissected, sliced into ~1 mm pieces and incubated at 37°C for 15 min in Hank's Balanced Salt Solution containing 0.3 mg/ml trypsin. Trypsin inhibitor was added to a final concentration of 0.5 mg/ml, and the tissue was mechanically dissociated by passing through a flame-polished Pasteur pipette. Cells were plated at 200,000-500,000 cells/cm^2 on plates coated with poly-L-lysine (0.1 mg/ml). Cells were maintained in Basal Medium Eagle supplemented with 10% dialyzed fetal bovine serum, penicillin/streptomycin, and KCl (25 mM). Cultures were used 4-7 days after plating. To reduce the number of non-neuronal cells in those cultures maintained for longer than 5 days, aphidicolin (3.3 mg/ml) was added to the medium 36 h after plating. Non-neuronal contamination of the cultures was assessed as described (25), and found to be less than 3%.

Proteasome inhibitors. PSI 1 was purchased from Calbiochem (La Jolla, CA) and was prepared as a stock solution in ethanol at 10 mM. MG132 was obtained from Sigma Chemical Co. (St. Louis, MO), and was prepared as a stock solution in DMSO at 10 mM. Control cell cultures were exposed to the vehicle only.

Antibodies. Monoclonal antibodies 3F4 (26) and 8H4 (27), and polyclonal antibody P45-66 (4) against PrP have been described previously. 3F4 was used to recognize transfected murine PrP in all immunoprecipitations and Western blots, except those involving stably transfected CHO cells expressing D177N PrP, in which P45-66 was used because the construct was not epitope-tagged. 8H4 was used for one of the

Downloaded from http://www.jbc.org/ by guest on March 24, 2020

Western blots shown in Fig. 5A to recognize both transfected murine PrP and endogenous rat PrP in PC12 cells.

An antibody (anti-SP) that selectively recognizes forms of murine PrP containing an uncleaved signal peptide was generated by immunizing rabbits with a synthetic peptide (TMWTDVGLCKKRPK; amino acids 14-27) that spans the signal peptide cleavage site at residues 22/23. The peptide was conjugated to KLH. This antibody shows no reactivity toward PrP molecules lacking the signal peptide, and its reactivity is completely blocked by incubation with the peptide immunogen. Detailed characterization of this antibody will be presented elsewhere (Stewart and Harris, manuscript in preparation). For immunofluorescence staining, the antibody was affinity-purified using immobilized peptide immunogen.

A monoclonal antibody to PDI was obtained from Stressgen Biotechnologies Corp. (Victoria, B.C.). Alexa 594-conjugated goat anti-mouse and Alexa 488-conjugated goat anti-rabbit IgGs were from Molecular Probes, Inc. (Eugene, OR). Anti-ubiquitin monoclonal antibody MAB1510 was purchased from Chemicon International (Temecula, CA).

Pulse-chase labeling and immunoprecipitation. Cells were incubated for 30 min in methionine- and cysteine-free medium prior to pulse-labeling in the same medium containing 250-750 μCi/ml of [^{35}S]methionine (Promix; Amersham Biosciences Corp., Piscataway, NJ). After washing, cells were chased in regular medium containing unlabeled methionine and cysteine for the indicated times. In some experiments, cycloheximide (100 μg/ml) was included in the chase medium to block completion of

Downloaded from http://www.jbc.org/ by guest on March 24, 2020

polypeptide chains that had been initiated but not completed during the pulse period (28). At the end of the chase period, cells were lysed in 0.5% SDS, 50 mM Tris-HCl (pH 7.5) containing protease inhibitors (pepstatin and leupeptin, 1 μg/ml; phenylmethylsulfonyl fluoride, 0.5mM; EDTA, 2 mM). The lysates were heated at 95°C for 5 min and then diluted 5-fold with 0.5% Triton X-100, 50 mM Tris-HCl (pH 7.5) containing protease inhibitors. PrP was then immunoprecipitated using the appropriate anti-PrP antibody and protein A-Sepharose beads, and analyzed by SDS-PAGE and autoradiography. In some cases, immunoprecipitated PrP was eluted from protein A-Sepharose beads at 95°C using 0.2% SDS, 50 mM Tris-HCl (pH 7.5), and subjected to treatment with endoglycosidase H (New England Biolabs, Beverly, MA) for 1 hr at 37°C. The radioactivity in PrP bands on gels was quantitated using a PhosphorImager SI or Storm 860 (Molecular Dynamics, Sunnyvale, CA). Background values measured in a region of the image that did not lie within the protein lanes were subtracted from each determination.

Western blots, Northern blots, and reverse transcriptase-PCR (RT-PCR). Western blots were performed as described previously (29). Films exposed using ECL were quantitated with SigmaScan Pro 5.0 (SPSS Science, Chicago, IL).

Total RNA was prepared using the RNA Wiz kit (Ambion Inc., Austin, TX). Northern blot analysis was performed using the Gene Images CDP-Star Chemiluminescent Detection System (Amersham). A 485 bp KpnI segment from the 3' end of the mouse PrP coding region was used as a probe. Under the hybridization conditions used in Fig. 5C, this probe cross-reacts with rat PrP mRNA.

Downloaded from http://www.jbc.org/ by guest on March 24, 2020

RT-PCR was performed using the TITANIUM one-step RT-PCR kit (Clontech, Palo Alto, CA). PrP primers (specific for mouse PrP mRNA) were as follows: sense, 5'-GGACCGCTACTACCGTGAAAAC-3'; anti-sense, 5'-TGGCCTGTAGTACACTTGGTTAGG-3'. Mouse β-actin primers were supplied by the manufacturer and were included in the same reaction to serve as an internal standard. Control reactions in which the RT was inactivated by heating at 95°C for 10 min showed no amplified bands. Aliquots were removed from the amplification reaction after 12, 16, and 20 cycles, and were analyzed by electrophoresis on 8% acrylamide /TBE gels followed by staining with SYBR Green I (Molecular Probes, Eugene, OR). Quantification of band intensities was performed on a Storm 860.

Topology and detergent insolubility assays. For determining the membrane topology of PrP, cells were lysed in 0.25 M sucrose, 10 mM HEPES (pH 7.4) by 10 passages through 27 gauge needles connected to 0.3 mm silastic tubing. After centrifugation at 2,300 x g for 2 min, the postnuclear supernatant was aliquoted into three tubes. One sample was left untreated; the second was digested with 250 ug/mL proteinase K for 30 min at 22°C in 50 mM Tris-HCl pH 7.5; and the third was digested with proteinase K in the presence of 0.5% Triton X-100 to solubilize membranes. Samples were precipitated with methanol and PrP analyzed by Western blotting.

To assay detergent insolubility, cells were lysed for 10 min on ice in 0.5% Triton X-100, 0.5% sodium deoxycholate, 50 mM Tris-HCl (pH 7.5). After debris was removed by centrifugation at 16,000 x g for 10 min, the supernatant was centrifuged at in a TLA 55 rotor at 186,000 x g for 40 min. Proteins in the supernatant were precipitated with

Downloaded from http://www.jbc.org/ by guest on March 24, 2020

methanol, and PrP in the supernatant and pellet fractions was analyzed by Western blotting.

Immunofluorescence staining. CHO cells plated on glass coverslips were fixed for 30 min in PBS containing 4% paraformaldehyde and 5% sucrose, and were then permeabilized for 10 min in PBS containing 0.05% Triton X-100. Cells were subsequently incubated at room temperature as follows: 30 min in PBS containing 2% goat serum (blocking buffer); 60 min with primary antibodies (anti-SP and anti-PDI) in blocking buffer; 15 min in blocking buffer; 60 min with Alexa-conjugated secondary antibodies in blocking buffer. Coverslips were mounted in 50% glycerol/PBS, and cells visualized by laser-scanning confocal microscopy using a Zeiss LSM-510 microscope.

Downloaded from http://www.jbc.org/ by guest on March 24, 2020

RESULTS

Maturation of mutant PrP molecules is delayed. We used pulse-chase labeling to analyze the maturation of newly synthesized PrP molecules in stably transfected CHO cells. We observed that WT PrP migrated as a major 33 kDa species immediately after pulse labeling (Fig. 1A, left panel). A 38 kDa form, which was barely visible at the end of the pulse period, increased in amount during the first 10 min of chase, and became the predominant species by 20 min. The 38 kDa form subsequently decayed with a half-life of ~3 hrs (see Fig. 3A). The 33 kDa species was shifted to a 25 kDa unglycosylated form after digestion with endoglycosidase H (endo H) (Fig. 1A, right panel). This shift indicates that that the 33 kDa band represents immature, core-

glycosylated molecules that had not yet transited beyond the mid-Golgi. In contrast, the 38 kDa form was resistant to endo H digestion, and thus represents mature, complex-glycosylated chains that have moved beyond the mid-Golgi to later compartments in the secretory pathway. In addition to the 38 kDa form, which is presumably glycosylated on both asparagine consensus sites, trace amounts of mature, singly glycosylated PrP (~32 kDa) can also be seen throughout the chase period. Quantitation of the bands revealed that a maximum of ~50-60% of radioactivity initially incorporated into the 33 kDa precursor during the pulse was eventually recovered in the mature, 38 kDa form. Thus, maturation of WT PrP molecules in CHO cells is rapid and efficient.

The maturation of PrP molecules carrying either of two pathogenic mutations was noticeably slower. PG14 is our designation for a nine-octapeptide insertion that is associated with a mixed phenotype in human beings having characteristics of both Creutzfeldt-Jakob disease and Gerstmann-Sträussler syndrome (12). PG14 PrP is initially synthesized as a 36 kDa form that matures into a 50 kDa species during the chase period (Fig. 1B, left panel). The 36 kDa form is shifted by digestion with endo H, confirming that it represents a core-glycosylated precursor, while the 50 kDa form is endo H-resistant (Fig. 1B, right panel). While the endo H-sensitive precursor of WT PrP has largely disappeared by 20 min of chase, the endo H-sensitive precursor of PG14 PrP is still present at 40 min of chase. Delayed maturation was also observed for PrP molecules carrying a second mutation, D177N/Met-128, which is linked to fatal familial insomnia (30) (Fig. 1C). In this case, the endo H-sensitive precursor (33 kDa) was still present after 20-30 min of chase.

Downloaded from http://www.jbc.org/ by guest on March 24, 2020

The slower maturation of the two mutant PrPs in comparison with WT PrP is clear from Fig. 1D, which plots the percentage of endo H-resistant PrP at different chase times. Of note, there was no appreciable difference between WT and mutant PrPs in the maximum amount of initial label that was chased into the endo H-resistant form (~50-60%), and in the half-life of this form (3-5 hrs; see Fig. 3A-C). Thus, mutant PrP molecules mature more slowly than WT PrP molecules in CHO cells, but the overall efficiency of maturation and the stability of the final product are similar for both types of PrP. We have seen a similar phenomenon when WT and PG14 PrPs are expressed in transiently transfected BHK cells (not shown).

To confirm that these observations held true for PrP molecules synthesized in neurons, we carried out pulse-chase labeling experiments on cerebellar granule cells cultured from transgenic mice expressing WT and PG14 PrP (12). We observed that WT PrP was fully endo H-resistant by 10-20 min of chase, while PG14 PrP required 40 min to become completely endo H-resistant (Fig. 2A, B). The delayed maturation of PG14 PrP is apparent when the percentage of endo H-resistant protein is quantitated (Fig. 2C). Despite this difference in the kinetics of maturation, there was no significant difference between WT and PG14 PrP in the maximum amount of initial label that was chased into the endo H-resistant form (~60-70%). These results demonstrate that the slower maturation of PG14 PrP compared to WT PrP is seen in neurons as well as in CHO and BHK cells.

Proteasome inhibitors do not alter the turnover or maturation of PrP. The pulse-chase data, combined with our previous morphological results (15), suggested

Downloaded from http://www.jbc.org/ by guest on March 24, 2020

that mutant PrP molecules are delayed in their transit along the early parts of the secretory pathway, probably including the ER. Since proteins retained in the ER are often rapidly degraded by the proteasome after retrotranslocation into the cytoplasm (20, 21), we wondered whether this degradative process might operate on mutant PrP molecules during their protracted residence in the ER. We therefore repeated the pulse-chase labeling experiments on CHO cells in the presence and absence of PSI 1 (Z-Ile-Glu(OtBu)-Ala-Leu-al), a peptide aldehyde which reversibly inhibits the chymotryptic activity of the proteasome. We observed that, in the absence of inhibitor, WT, PG14 and D177N PrP molecules had similar half-lives, ranging from 3-5 hrs (Fig. 3A-C). PSI 1 did not significantly prolong these half-lives (Fig. 3A-C). In addition, the inhibitor did not affect the kinetics with which the core-glycosylated precursor of each protein was converted to the mature form, and did not change the maximal percentage of the initial label that was chased into the mature form (~50-60%). We know that PSI 1 was active in these experiments, based on accumulation of high molecular mass, ubiquitin-protein conjugates detected on Western blots with an anti-ubiquitin antibody (data not shown). Results similar to those shown in Fig. 3 were obtained using lactacystin, an inhibitor which irreversibly blocks all three catalytic activities of the proteasome (data not shown). We conclude from these data that, although mutant PrP molecules are delayed in their exit from the ER, the majority of them are not substrates for proteasomal degradation following retrotranslocation. Our results do not rule out the possibility that a minority of PrP molecules are degraded by the latter pathway, since in this case a small effect of proteasome inhibitors on PrP half-life might be difficult to detect.

Downloaded from http://www.jbc.org/ by guest on March 24, 2020

Long-term treatment of transfected cells with proteasome inhibitors artifactually increases PrP mRNA and synthetic rate. Despite the fact that the inhibitor had no effect on PrP metabolism in pulse-chase experiments on CHO cells (Fig. 3), we found that it significantly increased the amount of both WT and mutant PrP observable by Western blotting of these cells (Fig. 4A). This effect was observable after 8 hrs of treatment, and was very dramatic after 18 hrs. In most cases, PSI 1 increased the amount of both glycosylated and unglycosylated PrP (Fig. 4A, PG14 and D177N), although in some cell clones the major species that accumulated was an unglycosylated form (Fig. 4A, WT). The glycosylated forms that accumulated in response to PSI 1 were resistant to endo H digestion (data not shown). The latter result was particularly surprising, since it seemed to imply that the proteasome was involved in degradation of fully mature PrP molecules that had already left the ER. Similar results were obtained with lactacystin (data not shown).

We suspected that some of these changes were due to secondary effects of PSI 1 that increased the synthetic rate of the protein, rather than to inhibition of the catalytic activity of the proteasome. This suspicion was confirmed by two lines of evidence. First, reverse transcriptase PCR analysis (Fig. 4B) and Northern blot analysis (data not shown) demonstrated that long-term exposure of CHO cells to PSI 1 significantly increased PrP mRNA levels. This effect varied among independent clones of transfected cells, with some clones showing as much as a 10-fold increase in PrP mRNA after overnight treatment with PSI 1. Second, PSI 1 increased the PrP synthetic rate, as measured by the amount of [^{35}S]methionine incorporated in a 20 min pulse (Fig.

Downloaded from http://www.jbc.org/ by guest on March 24, 2020

4C). Remarkably, treatment of cells with PSI 1 for as little as 2 hrs caused a progressive increase in PrP synthesis 2-4 hours after the inhibitor had been removed (Fig. 4C, lanes 4, 7, 8, 11, 12). These effects were not seen in the pulse-chase studies shown in Fig. 3, because in those experiments the cells had been treated with PSI 1 for only 30 min at the time of pulse-labeling, a time that would be too short to cause an increase in PrP synthesis.

Proteasome inhibitors also increased PrP protein and mRNA in stably transfected lines of PC12 cells that express WT or PG14 PrP. Fig. 5 shows the effect of the peptide aldehyde inhibitor MG132 (Z-Leu-Leu-Leu-al), and similar results were seen with ALLN (Ac-Leu-Leu-NorLeu-al) and lactacystin (data not shown). An increase in PrP mRNA was first apparent between 2 and 4 hrs (Fig. 5C, lanes 6-15; and Fig. 5D), and an increase in PrP protein by 4-8 hrs (Fig. 5A, top and middle panels, lanes 6-15; and Fig. 5B). We noted that MG132 did not have any effect on the levels of endogenous rat PrP (detected with 8H4 antibody) or its mRNA, as assayed in control PC12 cells that had been transfected with the empty expression vector lacking the murine PrP insert (Fig 5A and 5C, lanes 1-5; and Fig. 5B, D). This result suggested that the inhibitor might be selectively altering transcription from expression constructs carrying a heterologous promoter (CMV in this case).

A small percentage of PrP molecules is degraded by the proteasome before translocation into the ER. To minimize these artifactual effects on PrP mRNA levels and synthetic rate, we restricted treatments with proteasome inhibitors to 8 hrs or less, and also utilized pools of transiently transfected cells to avoid the clonal variation seen

Downloaded from http://www.jbc.org/ by guest on March 24, 2020

with stably transfected lines. Under these circumstances, the primary effect of PSI 1 was to cause the accumulation of a PrP species that was ~2 kDa larger than the corresponding mature, unglycosylated form (27 kDa for WT and D177N PrP and 33 kDa for PG14 PrP) (Fig. 6, lanes 2, 6, 10). The inhibitor-induced bands were not shifted by digestion with either endo H or PNGase F, and were also produced after PSI 1 treatment of cells synthesizing a form of PrP (T182/198A) in which both consensus sites for N-glycosylation had been mutated (data not shown). These results indicated that the PSI 1-induced species were not alternate glycoforms of PrP. In addition, we found that migration of the 27/33 kDa bands did not shift after treatment with PIPLC (not shown), indicating that they most likely lacked a C-terminal GPI anchor.

To explain why the 27/33 kDa bands induced by PSI 1 were slightly larger in size than mature, unglycosylated PrP, we hypothesized that they contained an intact signal peptide. To directly test this hypothesis, we reacted Western blots with an antibody (anti-SP) that specifically recognizes the PrP signal peptide. We found that the 27/33 kDa bands were selectively labeled with this antibody (Fig. 6, lanes 4, 8, 12). Thus, these bands represent unprocessed forms of PrP that are not glycosylated and from which the signal peptide has not been removed. The fact that these forms accumulate in the presence of PSI 1 indicates that they are normally degraded by the proteasome. We noted that small amounts of the signal peptide-containing forms were sometimes detectable even in the absence of PSI 1 (Fig. 6, lanes 9 and 11). This phenomenon appeared to correlate with the level of PrP expression in a particular transfection experiment, rather than with the PrP sequence being expressed (data not shown). Accumulation of unglycosylated, signal-peptide containing forms of WT and PG14 PrP

Downloaded from http://www.jbc.org/ by guest on March 24, 2020

was also observed after proteasome inhibitor treatment of transfected PC12 cells (Fig. 5A, bottom panel, lanes 6-15).

To further analyze the metabolism of the signal peptide-bearing form, we carried out pulse-chase labeling of transiently transfected CHO cells expressing WT PrP in the presence and absence of proteasome inhibitor, and then subjected cell lysates to immunoprecipitation using either 3F4 or anti-SP antibodies. In untreated cells, the 3F4 antibody recognized glycosylated bands at 32-38 kDa, as well as an unglycosylated band of 25 kDa (Fig. 7A, left panel). In the presence of PSI 1, a band of 27 kDa appeared (Fig. 7A, right panel), corresponding to the additional species observed on Western blots of cells treated with inhibitor (Fig. 6, lane 2). As expected, only the 27 kDa band was immunoprecipitated by the anti-SP antibody, confirming its identity as an unprocessed, signal peptide-containing form of PrP (Fig. 7B, right panel). Untreated cells contained lower levels of the 27 kDa form, which could be visualized by immunoprecipitation with anti-SP antibody (Fig. 7B, left panel). Of note, the half-life of the 27 kDa form was very short ($t_{½}$ = 30 min) in untreated cells, and was significantly extended (to ~4 hrs) by including PSI 1 in the chase medium (Fig. 7D), consistent with the conclusion that this form is normally degraded by the proteasome. The fact that PSI 1 increased the amount of the 27 kDa form that was present at the start of the chase period implies that this species undergoes significant proteasomal degradation even within the 20 min period of pulse labeling (compare 0 hr lanes in the left and right panels of Fig. 7B). In contrast, the rest of the PrP species (including both unglycosylated and glycosylated forms lacking a signal peptide) had a half-life of ~3 hrs, and this value was

Downloaded from http://www.jbc.org/ by guest on March 24, 2020

not affected by PSI 1 (Fig. 7C). The latter result is similar to what was observed in experiments on stably transfected cells (Fig. 3).

The presence of the signal peptide on the 27 kDa form of PrP that accumulates in the presence of proteasome inhibitor suggested that this polypeptide had not yet been translocated into the ER lumen where signal peptidase is located. To directly probe the topology of the 27 kDa form, we carried out a protease protection assay on microsomes prepared from control and inhibitor-treated cells synthesizing WT PrP. We found that the 27 kDa band was selectively degraded by protease treatment of intact microsomes, while other PrP forms (both glycosylated and unglycosylated), were protected (Fig. 8A). This result implies that the 27 kDa polypeptide is present on the cytoplasmic side of the ER membrane. We also observed that, in contrast to the other PrP forms, the untranslocated polypeptide was insoluble in non-ionic detergents (Fig. 8B).

To determine the localization of the 27 kDa form in intact cells, we carried out immunofluorescence staining of CHO cells expressing WT PrP using anti-SP antibody and an antibody to protein disulfide isomerase (PDI) as a marker for the ER. We observed very little staining with anti-SP antibody in untreated cells (Fig. 9A). Treatment with PSI 1 caused marked accumulation of anti-SP-reactive PrP in an intracellular distribution that colocalized with PDI (Fig. 9D-F). In conjunction with the results of the topology assay, the immunofluorescence data imply that the signal peptide-bearing form of PrP that accumulates in the presence of proteasome inhibitors is closely associated with the cytoplasmic surface of the ER membrane.

Downloaded from http://www.jbc.org/ by guest on March 24, 2020

Taken together, our data indicate that a fraction of newly synthesized PrP molecules are never translocated or processed. These chains are normally degraded by the proteasome, probably in close apposition to the cytoplasmic surface of the ER membrane.

Proteasome inhibitors do not cause accumulation of PrP in cerebellar granule neurons. We found that treatment of neurons expressing either WT or PG14 PrP with MG132 for up to 8 hrs had no effect on any of the PrP bands seen by Western blotting using 3F4 antibody, including both glycosylated and unglycosylated species (Fig. 10A, B, upper panels). Blots of the same cell lysates developed with an anti-ubiquitin antibody revealed accumulation of high molecular mass, ubiquitinated proteins, demonstrating the efficacy of the inhibitor treatment (Fig. 10A, B, lower panels). PrP levels decreased after 24 hrs of exposure, but this is likely due to the death of a significant proportion of the neurons that had occurred by this time (data not shown). Prolonged treatment of cerebellar granule neurons with proteasome inhibitors is known to induce apoptosis (31). Results similar to those shown in Fig. 10A, B were obtained with other inhibitors, including ALLN (50-200 μM), lactacystin (0.1-10 μM), and lactacystin β-lactone (10 μM), and with neurons from non-transgenic C57BL/6J mice (data not shown).

Blotting of the same samples from MG132-treated neurons with anti-SP antibody failed to reveal the presence of signal peptide-bearing forms of either WT or PG14 PrP (Fig. 10C, lanes 1-12). Lysates from transfected PC12 cells treated with MG132 for 24 hrs were used to provide markers for the sizes of the signal peptide-containing forms

Downloaded from http://www.jbc.org/ by guest on March 24, 2020

(27 for WT and 33 kDa for PG14) (Fig. 10C, lane 13). The faint bands seen at 27 kDa after inhibitor treatment of neurons expressing WT PrP (Fig. 10C, upper panel, lanes 11 and 12) are likely to be non-specific, since they were not apparent in the blot developed with 3F4 antibody (Fig. 10A, upper panel, lanes 11 and 12), and since we did not observe them in every experiment. We also failed to see PrP forms reactive with anti-SP antibody after metabolic labeling of cerebellar granule neurons (data not shown). We conclude that PrP is not subject to proteasomal degradation in these neurons, either before translocation or after retrotranslocation.

DISCUSSION

The present work addresses a question that has become a recent focus of interest in the prion field: how is PrP synthesized and metabolized by the cell, and how might pathogenic mutations alter these processes? We demonstrate here that PrP molecules carrying disease-associated mutations are significantly delayed in their transit along the early part of the secretory pathway. This phenomenon appears to be a general feature of the biosynthesis of at least a subset of mutant PrPs, since it is observed with two different mutations, and is apparent in transfected CHO and BHK cells, as well as in cultured neurons from transgenic mice. We find that, in contrast to some other secretory proteins that misfold during their biosynthesis, mutant PrPs are not subject to ER-associated degradation, involving retrotranslocation into the cytoplasm and then degradation by the proteasome. A small number of PrP molecules, both mutant and WT, are degraded by the proteasome, but these represent aberrant

Downloaded from http://www.jbc.org/ by guest on March 24, 2020

chains that have been translated in the cytoplasm, but have not been translocated into the ER lumen. Our results strongly contrast with those of two other groups that have recently claimed a role for the proteasome in the degradation of retrotranslocated PrP.

Mutant PrP is delayed in its exit from the ER. N-linked oligosaccharide chains become resistant to cleavage by endo H in the mid-Golgi, as a result of the action of Golgi mannosidase II. The slower maturation of mutant PrPs from an endo H-sensitive to an endo H-resistant form therefore suggests that these proteins transit the early part of the secretory pathway more slowly than WT PrP. This observation is consistent with a previous study in which we localized mutant PrP molecules in transfected cells using immunofluorescence and immunoelectron microscopy, and by florescence microscopy of PrP-EGFP fusion proteins (15). We found that several different mutant PrPs, including PG14 and D177N, were present on the cell surface at reduced levels compared to WT PrP. In addition, many cells showed accumulation of mutant PrP in the ER. Similar observations regarding the cellular distribution of mutant PrPs have been made by several other laboratories (9, 32-35). The combined results of localization and biosynthetic studies therefore suggest that mutant PrP molecules are delayed in their export from the ER. This delay results in a steady-state distribution in which the proteins are concentrated in the ER, and are expressed at lower levels on the cell surface. Although it was originally thought that exit of newly synthesized proteins from the ER was a default process, it is now clear that a number of factors may influence the anterograde transport rate (36-38). These include the kinetics of polypeptide chain folding, association with ER chaperones, interaction with cargo

Downloaded from http://www.jbc.org/ by guest on March 24, 2020

receptors and coat proteins in ER transport vesicles, binding to specific ligands, and self-aggregation. One or more of these factors may play a role in retarding transit of mutant PrPs out of the ER.

The role of the proteasome in PrP degradation. Secretory or membrane proteins that are retained in the ER are sometimes subject to a quality control process in which they are retrotranslocated into the cytoplasm and degraded by the proteasome (20, 21). This mechanism is meant to ensure that abnormally folded proteins, or those that are not properly modified or assembled into multi-subunit complexes, do not reach the plasma membrane where they might cause cellular damage. Several pieces of evidence presented here argue strongly that the majority of PrP molecules, both mutant and WT, are not subject to ER-associated degradation involving the proteasome. First, proteasome inhibitors do not affect the half-life of WT or mutant PrPs in pulse-chase experiments. Second, the inhibitors do not alter the kinetics with which core-glycosylated precursors of PrP are converted to mature, endo H-resistant forms. Third, the percentage of the initial radioactive label that is chased into mature forms is high (50-70%), and is not influenced by the presence of proteasome inhibitors. If significant numbers of PrP molecules were being degraded by the proteasome after retrotranslocation from the ER, then proteasome inhibitors would be expected to rescue disappearance of immature forms early in the chase period, resulting in an increase in the half-life and in the steady state levels of the protein. These effects have been observed for other proteins, such as T-cell receptor α-chain (39), MHC class I heavy chain (40), Ig light chain (41), and α_1-antitrypsin Z (42) that are known to be substrates

Downloaded from http://www.jbc.org/ by guest on March 24, 2020

for retrotranslocation and proteasomal degradation. Cystic fibrosis transmembrane regulator (CFTR), the classic example of a protein subject to ER-associated degradation, is also stabilized by proteasome inhibitors in pulse-chase experiments, although in this case it is high molecular weight, ubiquitinated intermediates that accumulate (43). For some substrates, proteasome inhibitors cause accumulation of retrotranslocated forms that have been stripped of their oligosaccharide chains by cytoplasmic glycosidases (39, 40). In contrast, the primary form of PrP that we observe after short-term treatment of cells with inhibitors is a signal peptide-bearing species that has most likely never been translocated or glycosylated (see below).

In contrast to the two PrP mutants we have analyzed here (one insertional and one missense), two stop codon mutants (Y145stop, Q160stop) do appear to be degraded primarily by the retrotranslocation/proteasome pathway. These molecules are turned over rapidly, are stabilized by proteasome inhibitors, and are found to accumulate intracellularly in the cytoplasm and nucleus under some circumstances (10, 44). Presumably, the absence of the C-terminal part of the polypeptide chain and the GPI anchor causes these mutants to interact with the ER quality control machinery in a way that full-length molecules do not.

Our results demonstrate that a small fraction of PrP molecules, both wild-type and mutant, is subject to proteasomal degradation in transfected cells by a pathway that does not involve retrotranslocation from the ER lumen. Proteasome inhibitors cause the selective accumulation of a form of PrP (27 kDa for WT and D177N, and 33 kDa for PG14) that is approximately 2 kDa larger than the mature, unglycosylated species. This form, which is the major one that accumulates on Western blots after short-term

Downloaded from http://www.jbc.org/ by guest on March 24, 2020

treatment of cells with proteasome inhibitors (≤ 8 hrs), is turned over rapidly ($t_{½}$ = 30 min), and its half-life is significantly prolonged by the inhibitors. Our data strongly suggest that the 27/33 kDa forms represent PrP molecules that reside on the cytoplasmic face of the ER membrane, and that have never been translocated into the lumen for further processing. The most decisive observation is that these species react with an antibody that is specific for PrP molecules bearing an intact signal peptide. This feature indicates that the proteins have not been exposed to signal peptidase, which resides in the lumen of the ER. The presence of the signal peptide argues persuasively against the possibility that the 27/33 kDa forms are delivered to the cytoplasm by a process of retrotranslocation, since in that case the signal peptide would have been removed during cotranslational insertion into the ER lumen. In addition, the 27/33 kDa forms lack N-linked glycans and a GPI anchor, based on the fact that their migration is not shifted by treatment with glycosidases or PIPLC. These features are consistent with lack of processing by oligosaccharyl transferase and GPI transamidase, both of which reside in the ER lumen. Topology analysis using a protease protection assay demonstrates directly that the 27 kDa protein is located entirely on the cytoplasmic side of the ER membrane. Finally, immunolocalization studies indicate that the 27 kDa form accumulates in an ER pattern after proteasome inhibitor treatment. Taken together, our results indicate that a small fraction of PrP chains fail to be translocated into the ER lumen during their synthesis, and these remain closely associated with the cytoplasmic face of the ER membrane where they are rapidly degraded by the proteasome. We suspect that these chains are ubiquitinated prior to proteasomal attack, since we have sometimes observed a ladder of higher molecular mass PrP species above the 27/33

Downloaded from http://www.jbc.org/ by guest on March 24, 2020

kDa band, with steps separated by ~8 kDa, after treatment of cells with proteasome inhibitors (data not shown). The phenomenon of abortive translocation we have observed here is not unique to PrP, and we think it is likely to reflect saturation of one or more components of the translocation machinery at the elevated expression levels typical of transfected cells. Untranslocated PrP does not accumulate in cultured cerebellar granule cells treated with proteasome inhibitors, implying that this species is unlikely to be an obligate by-product of PrP biosynthesis in neurons. Untranslocated, signal peptide-bearing forms of other proteins have been found to accumulate in transfected cells treated with proteasome inhibitors (39).

Artifactual effects of proteasome inhibitors. We have uncovered a previously unappreciated side-effect of proteasome inhibitors. Although the toxic and stress-inducing effects of these drugs are well known, we have found that proteasome inhibitors are also capable of increasing the synthesis of a specific protein, PrP, and its mRNA in transfected cells. Preliminary experiments indicate that the inhibitors may have a similar effect on other heterologously expressed proteins (R.C. and E.B., unpublished data). The effect of proteasome inhibitors on PrP mRNA and synthetic rate first became apparent after 2-4 hrs of treatment, and was very marked after 18-24 hrs. Our evidence suggests that the effect is related to the CMV promoter driving expression of PrP, since proteasome inhibitors did not alter levels of PrP protein or mRNA derived from the endogenous rat gene in PC12 cells, or from the mouse PrP gene (either endogenous or carried on a transgene) in cultured neurons. The mechanism underlying this unexpected effect of proteasome inhibitors could be related to stabilization of the

Downloaded from http://www.jbc.org/ by guest on March 24, 2020

turnover of transcription or translation factors, or to activation of signaling pathways that impinge on transcription from the CMV promoter (45-48). Since the effect varied between different clones of stably transfected cells, it seems likely that the insertion site in the chromatin could also play a role. Whatever its cause, this potential artifact is important to bear in mind when interpreting experiments using proteasome inhibitors, particularly those involving expression of proteins from heterologous promoters, and those in which the drugs are applied for extended periods of time.

The role of ER accumulation in disease pathogenesis. A number of inherited human diseases are attributable to defects in export of a mutant protein from the ER (22, 36, 49, 50). In some cases, such as cystic fibrosis and hereditary hemochromatosis, the mutant protein is retrotranslocated from the ER and degraded by the proteasome, resulting in failure of the protein to reach its normal cellular destination. In other disorders, such as hereditary emphysema (PiZ variant) and congenital hypothyroidism, the retained protein accumulates in the ER without being degraded. In these cases, the disease phenotype is due to a toxic effect of the accumulated protein, which stimulates one or more ER stress response pathways. Based on the data presented here, we hypothesize that some inherited prion disorders, such as those due to PG14 and D177N, are members of this second category of ER retention diseases. Although transit of these mutant PrP molecules out of the ER is not completely blocked, their export rate is reduced sufficiently to cause an accumulation of the protein in the ER at steady state. We are currently investigating whether build-up of mutant PrP in the ER activates pro-apoptotic stress pathways. Regardless of the pathway involved, it is clear

Downloaded from http://www.jbc.org/ by guest on March 24, 2020

that PG14 PrP is a potent trigger of neuronal death, since transgenic mice expressing this protein develop a fatal neurodegenerative illness characterized by massive apoptosis of cerebellar granule cells (11, 12).

Comparison with other studies. Our results require a major shift in the interpretation of several previously published studies on the role of the proteasome in the metabolism of PrP. Two other laboratories have reported that proteasome inhibitors cause the accumulation of a 26-27 kDa, unglycosylated form of wild-type PrP in several different cultured cell types (17, 19). The accumulated PrP was present in the cytoplasm by immunofluorescence staining, partially colocalizing with the cytoplasmic heat shock protein Hsc70 (17). Based on the fact that the 26 kDa species migrated on SDS-PAGE at the position of recombinant PrP 23-230, it was suggested that this form was processed at both the N- and C-termini (i.e., the signal peptide and GPI addition sequence had been removed in the ER) (17). These authors therefore concluded that a population of PrP molecules was normally subject to retrotranslocation into the cytoplasm after insertion into the ER lumen, followed by rapid proteasomal degradation. The absence of oligosaccharide chains on the retrotranslocated molecules was suggested to be due to the action of cytoplasmic glycosidases.

In contrast, our results make it clear that the unglycosylated PrP molecules that accumulate after proteasome treatment are not fully processed polypeptide chains derived by retrotranslocation. Rather, they are abortive translocation products that have never left the cytoplasm, and that therefore have intact signal peptides and GPI addition sequences. These molecules represent a relatively small fraction of the total PrP

Downloaded from http://www.jbc.org/ by guest on March 24, 2020

chains synthesized, and their production is associated with high expression levels in transfected cells. The fact that, in our hands, short-term treatment of cells with proteasome inhibitors has no consistent effect other than stabilization of this untranslocated species indicates that neither wild-type or mutant PrP molecules are major substrates for degradation by ER quality control mechanisms. Similar to Yedidia et al. (19), we find that long-term inhibitor treatment causes accumulation of mature, glycosylated PrP forms, but this effect is very likely attributable to the artifactual increase in PrP mRNA and synthetic rate that we have shown occurs under these conditions.

It has been suggested that some of the cytoplasmic PrP that accumulates in the presence of proteasome inhibitors has been converted to a PrP^{Sc}-like conformation, based on its detergent insolubility and protease resistance (18, 51). In support of the claim that this conformation is self-perpetuating (infectious), it was reported that aggregated and protease-resistant PrP continued to accumulate in transfected cells for a number of hours after removal of proteasome inhibitors (18). In light of the results reported here, however, we would offer an alternative explanation for this result. We suggest that the initial inhibitor treatment caused a sustained increase in the synthesis of PrP which continued even after the inhibitor was removed. This is the same phenomenon that we have illustrated in Fig. 4C, and is likely to result in the accumulation of multiple forms of PrP, including glycosylated, unglycosylated, and untranslocated species. Thus, increased PrP synthesis, rather than a self-propagating conformational change, probably accounts for the continued accumulation of PrP after transient treatment with proteasome inhibitors.

Downloaded from http://www.jbc.org/ by guest on March 24, 2020

On the basis of several kinds of observations in both cultured cells and transgenic mice, it has been proposed that cytosolic PrP is highly cytotoxic, and that accumulation of this form may represent the first step in a pathogenic cascade operative in both inherited and infectiously acquired prion diseases (23). While the results reported here argue strongly against retrotranslocation as a mechanism for generation of cytosolic PrP, they do not address the potential toxicity of PrP that might accumulate in the cytoplasm as a result of other processes, for example abortive translocation. It has been reported that artificial targeting of PrP to the cytoplasm by deletion of the N-terminal signal sequence is toxic to transfected cells and transgenic mice (23). However, in the absence of evidence that cytosolic PrP increases during the course of a natural prion disease, it is difficult to be certain of the pathogenic role of this form. Our data argue that accumulation of misfolded forms of mutant PrP in the lumen of the ER, rather than in the cytoplasm, represents a more likely instigating event in at least a subset of inherited prion disorders.

Downloaded from http://www.jbc.org/ by guest on March 24, 2020

ACKNOWLDEGMENTS

We thank Gianluigi Zanusso and Man-Sun Sy for 8H4 antibody, as well as Richard Kascsak for 3F4 antibody. We also acknowledge Michael Green for critical reading of the manuscript.

Downloaded from http://www.jbc.org/ by guest on March 24, 2020

REFERENCES

1. Prusiner, S. B. (1998) *Proc. Natl. Acad. Sci. USA* **95**, 13363-13383
2. Collinge, J. (2001) *Annu. Rev. Neurosci.* **24**, 519-550
3. Young, K., Piccardo, P., Dlouhy, S., Bugiani, O., Tagliavini, F., and Ghetti, B. (1999) in *Prions: Molecular and Cellular Biology* (Harris, D. A., ed), pp. 139-175, Horizon Scientific Press, Wymondham, UK
4. Lehmann, S., and Harris, D. A. (1995) *J. Biol. Chem.* **270**, 24589-24597
5. Lehmann, S., and Harris, D. A. (1996) *J. Biol. Chem.* **271**, 1633-1637
6. Lehmann, S., and Harris, D. A. (1996) *Proc. Natl. Acad. Sci. USA* **93**, 5610-5614
7. Chiesa, R., and Harris, D. A. (2000) *J. Neurochem.* **75**, 72-80
8. Priola, S. A., and Chesebro, B. (1998) *J. Biol. Chem.* **273**, 11980-11985
9. Singh, N., Zanusso, G., Chen, S. G., Fujioka, H., Richardson, S., Gambetti, P., and Petersen, R. B. (1997) *J. Biol. Chem.* **272**, 28461-28470
10. Lorenz, H., Windl, O., and Kretzschmar, H. A. (2002) *J. Biol. Chem.* **277**, 8508-8516
11. Chiesa, R., Drisaldi, B., Quaglio, E., Migheli, A., Piccardo, P., Ghetti, B., and Harris, D. A. (2000) *Proc. Natl. Acad. Sci. USA* **97**, 5574-5579
12. Chiesa, R., Piccardo, P., Ghetti, B., and Harris, D. A. (1998) *Neuron* **21**, 1339-1351
13. Daude, N., Lehmann, S., and Harris, D. A. (1997) *J. Biol. Chem.* **272**, 11604-11612
14. Narwa, R., and Harris, D. A. (1999) *Biochemistry* **38**, 8770-8777
15. Ivanova, L., Barmada, S., Kummer, T., and Harris, D. A. (2001) *J. Biol. Chem.* **276**, 42409-42421

Downloaded from http://www.jbc.org/ by guest on March 24, 2020

16. Stewart, R. S., Drisaldi, B., and Harris, D. A. (2001) *Mol. Biol. Cell* **12**, 881-889.

17. Ma, J., and Lindquist, S. (2001) *Proc. Natl. Acad. Sci. USA* **98**, 14955-14960

18. Ma, J., and Lindquist, S. (2002) *Science* **298**, 1785-1788

19. Yedidia, Y., Horonchik, L., Tzaban, S., Yanai, A., and Taraboulos, A. (2001) *EMBO J.* **20**, 5383-5391

20. Bonifacino, J. S., and Weissman, A. M. (1998) *Annu. Rev. Cell Dev. Biol.* **14**, 19-57

21. Tsai, B., Ye, Y., and Rapoport, T. A. (2002) *Nat. Rev. Mol. Cell Biol.* **3**, 246-255

22. Aridor, M., and Hannan, L. A. (2000) *Traffic* **1**, 836-851

23. Ma, J., Wollmann, R., and Lindquist, S. (2002) *Science* **298**, 1781-1785

24. Lehmann, S., and Harris, D. A. (2000) *J. Biol. Chem.* **275**, 1520

25. Miller, T. M., and Johnson, E. M., Jr. (1996) *J. Neurosci.* **16**, 7487-7495

26. Kascsak, R. J., Rubinstein, R., Merz, P. A., Tonna-DeMasi, M., Fersko, R., Carp, R. I., Wisniewski, H. M., and Diringer, H. (1987) *J. Virol.* **61**, 3688-3693

27. Zanusso, G., Liu, D., Ferrari, S., Hegyi, I., Yin, X., Aguzzi, A., Hornemann, S., Liemann, S., Glockshuber, R., Manson, J. C., Brown, P., Petersen, R. B., Gambetti, P., and Sy, M. S. (1998) *Proc. Natl. Acad. Sci. USA* **95**, 8812-8816

28. Braakman, I., Hoover-Litty, H., Wagner, K. R., and Helenius, A. (1991) *J. Cell Biol.* **114**, 401-411

29. Harris, D. A., Huber, M. T., van Dijken, P., Shyng, S.-L., Chait, B. T., and Wang, R. (1993) *Biochemistry* **32**, 1009-1016

30. Goldfarb, L. G., Petersen, R. B., Tabaton, M., Brown, P., LeBlanc, A. C., Montagna, P., Cortelli, P., Julien, J., Vital, C., Pendelbury, W. W., Haltia, M., Wills, P. R., Hauw, J. J., McKeever, P. E., Monari, L., Schrank, B., Swergold, G. D., Autilio-

Downloaded from http://www.jbc.org/ by guest on March 24, 2020

Gambetti, L., Gajdusek, D. C., Lugaresi, E., and Gambetti, P. (1992) *Science* **258**, 806-808

31. Porcile, C., Piccioli, P., Stanzione, S., Bajetto, A., Bonavia, R., Barbero, S., Florio, T., and Schettini, G. (2002) *Ann. N.Y. Acad. Sci.* **973**, 402-413
32. Jin, T., Gu, Y., Zanusso, G., Sy, M., Kumar, A., Cohen, M., Gambetti, P., and Singh, N. (2000) *J. Biol. Chem.* **275**, 38699-38704.
33. Capellari, S., Parchi, P., Russo, C. M., Sanford, J., Sy, M.-S., Gambetti, P., and Petersen, R. B. (2000) *Am. J. Pathol.* **157**, 613-622.
34. Petersen, R. B., Parchi, P., Richardson, S. L., Urig, C. B., and Gambetti, P. (1996) *J. Biol. Chem.* **271**, 12661-12668
35. Negro, A., Ballarin, C., Bertoli, A., Massimino, M. L., and Sorgato, M. C. (2001) *Mol. Cell. Neurosci.* **17**, 521-538.
36. Aridor, M., and Balch, W. E. (1999) *Nat. Med.* **5**, 745-751
37. Aridor, M., and Balch, W. E. (2000) *Science* **287**, 816-817
38. Aridor, M., and Balch, W. E. (1996) *Trends Cell Biol.* **6**, 315-320
39. Yu, H., Kaung, G., Kobayashi, S., and Kopito, R. R. (1997) *J. Biol. Chem.* **272**, 20800-20804
40. Wiertz, E. J., Jones, T. R., Sun, L., Bogyo, M., Geuze, H. J., and Ploegh, H. L. (1996) *Cell* **84**, 769-779
41. O'Hare, T., Wiens, G. D., Whitcomb, E. A., Enns, C. A., and Rittenberg, M. B. (1999) *J. Immunol.* **163**, 11-14
42. Qu, D., Teckman, J. H., Omura, S., and Perlmutter, D. H. (1996) *J. Biol. Chem.* **271**, 22791-22795

Downloaded from http://www.jbc.org/ by guest on March 24, 2020

43. Gelman, M. S., Kannegaard, E. S., and Kopito, R. R. (2002) *J. Biol. Chem.* **277**, 11709-11714

44. Zanusso, G., Petersen, R. B., Jin, T., Jing, Y., Kanoush, R., Ferrari, S., Gambetti, P., and Singh, N. (1999) *J. Biol. Chem.* **274**, 23396-23404

45. Nakayama, K., Furusu, A., Xu, Q., Konta, T., and Kitamura, M. (2001) *J. Immunol.* **167**, 1145-1150

46. Kawazoe, Y., Nakai, A., Tanabe, M., and Nagata, K. (1998) *Eur. J. Biochem.* **255**, 356-362

47. Zimmermann, J., Erdmann, D., Lalande, I., Grossenbacher, R., Noorani, M., and Furst, P. (2000) *Oncogene* **19**, 2913-2920

48. Wu, H. M., Wen, H. C., and Lin, W. W. (2002) *Am. J. Respir. Cell Mol. Biol.* **27**, 234-243

49. Kim, P. S., and Arvan, P. (1998) *Endocr. Rev.* **19**, 173-202

50. Aridor, M., and Hannan, L. A. (2002) *Traffic* **3**, 781-790

51. Ma, J., and Lindquist, S. (1999) *Nature Cell Biol.* **1**, 358-361

Downloaded from http://www.jbc.org/ by guest on March 24, 2020

FIGURE LEGENDS

FIGURE 1: Biosynthetic maturation of mutant PrP to an endo H-resistant form in CHO cells is delayed. Stably transfected CHO cells expressing **(A)** WT PrP, **(B)** PG14 PrP, or **(C)** D177N PrP were pulse-labeled with [^{35}S]methionine for 20 min, and then chased in medium containing unlabeled methionine for 0, 10, 20, 30, 40, 60, or 90 min. Cells were then lysed, and PrP was isolated by immunoprecipitation. Half of the immunoprecipitated PrP was treated with endo H (gels on the right) and half was left untreated (gels on the left) prior to analysis by SDS-PAGE and autoradiography. The black and white arrows and the shaded arrowhead indicate, respectively, the positions of mature (endo H-resistant), immature (endo H-sensitive), and unglycosylated PrP. Molecular mass markers are given in kilodaltons. **(D)** The percentage of endo H-resistant PrP at each chase time was calculated from PhosphorImager analysis of the gels shown in panels A-C, using the formula {1 – [(X-Y)/T]} x 100, where X = amount of unglycosylated PrP after treatment with endo H; Y = amount of unglycosylated PrP without endo H treatment; T = total PrP. Values were scaled to 0% and 100% endo H-resistance at 0 and 90 min, respectively, to correct for the efficiency of endo H cleavage. The results are representative of 5 independent experiments.

FIGURE 2: Biosynthetic maturation of PG14 PrP to an endo H-resistant form in neurons is delayed. Cerebellar granule neurons cultured from transgenic mice expressing **(A)** WT PrP or **(B)** PG14 PrP were pulse-labeled with [^{35}S]methionine for 20 min, and then chased in medium containing unlabeled methionine for 0, 10, 20,

Downloaded from http://www.jbc.org/ by guest on March 24, 2020

40, 60, or 300 min. Cells were then lysed, and PrP was isolated by immunoprecipitation. Half of the immunoprecipitated PrP was treated with endo H (gels on the right) and half was left untreated (gels on the left) prior to analysis by SDS-PAGE and autoradiography. The black and white arrows and the shaded arrowhead indicate the positions, respectively, of mature (endo H-resistant), immature (endo H-sensitive), and unglycosylated PrP. **(C)** The percentage of endo H-resistant PrP at each chase time was calculated from PhosphorImager analysis of the gels shown in panels A and B, using the formula given in the legend to Fig. 1D. The results are representative of 2 independent experiments.

FIGURE 3: Proteasome inhibition does not alter the half-lives of WT or mutant PrPs. Stably transfected CHO cells expressing **(A)** WT PrP, **(B)** PG14 PrP, or **(C)** D177N PrP were pulse-labeled with [^{35}S]methionine for 20 min, and then chased in medium containing unlabeled methionine for the indicated times (in min). In one set of cultures (gels on the right), PSI-1 (20 μM) was present during a 30 min pre-incubation, as well as during the pulse and chase periods. In the other set of cultures (gels on the left), an equivalent amount of ethanol vehicle was present. At the end of the chase period, cells were lysed, and PrP was isolated by immunoprecipitation and analyzed by SDS-PAGE and autoradiography. The black and white arrows indicate the positions, respectively, of mature (endo H-resistant) and immature (endo H-sensitive) PrP. The graphs show semi-logarithmic plots of the percentage of initial label present in both PrP bands (mature + immature) at each chase time. Each circle represents an independent

Downloaded from http://www.jbc.org/ by guest on March 24, 2020

experiment. The lines were fitted by least-squares analysis to obtain the half-life ± S.E.M.

FIGURE 4: Long-term treatment of CHO cells with a proteasome inhibitor increases PrP protein, mRNA, and synthetic rate. (A) Stably transfected CHO cells expressing WT, PG14, D177N PrPs were treated with PSI 1 (20 μM) for the indicated times. Cells were then lysed, and PrP analyzed by Western blotting. The arrow points to an unglycosylated form of WT PrP that is increased by PSI 1 treatment. **(B)** The same cell lines used in (A) were treated with PSI 1 for the indicated times, and then PrP and β-actin mRNA were analyzed by RT-PCR. Samples were removed after 16 and 20 cycles of amplification to assess saturation of the signal. Size markers are in nucleotides. **(C)** Stably transfected CHO cells expressing WT PrP were either treated with ethanol vehicle for 10 hrs (lanes 1, 5, 9), or were incubated with PSI 1 for 2 hrs (lanes 2-4), 4 hrs (lanes 6-8), or 6 hrs (lanes 10-12). At the end of the PSI 1 incubation, cells were either analyzed immediately (lanes 2, 6, 10), or were transferred to inhibitor-free medium for 2 hr (lanes 3, 7, 11) or 4 hrs (lanes 4, 8, 12). At the end of all incubations, cells were pulse-labeled with [^{35}S]methionine for 20 min, after which PrP was immunoprecipitated and analyzed by SDS-PAGE and autoradiography. Autoradiographic analysis of lysates prior to immunoprecipitation revealed equal incorporation of [^{35}S]methionine into total cellular proteins in all samples (not shown).

FIGURE 5: Long-term treatment of PC12 cells with a proteasome inhibitor increases PrP protein and mRNA. (A) PC12 cells stably transfected with the empty

Downloaded from http://www.jbc.org/ by guest on March 24, 2020

expression vector (lanes 1-5), or with the vector encoding WT murine PrP (lanes 6-10) or PG14 murine PrP (lanes 11-15) were exposed to MG132 (10 μM) for the indicated times. Cells were then lysed, and PrP analyzed by Western blotting using either 3F4 antibody (top panel) which detects only epitopically tagged murine PrP; 8H4 antibody (middle panel) which detects both murine PrP and endogenous rat PrP; or anti-SP antibody (bottom panel) which detects signal peptide-bearing forms of murine PrP. For the 8H4 blot, a longer exposure is shown for lanes 1-5 than for the other lanes. The black and white arrowheads to the right of the bottom panel indicate the positions, respectively, of WT and PG14 PrP containing an uncleaved signal peptide. **(B)** The PrP signals from the 8H4 blot shown in (A) were quantitated, and expressed relative to the amount of PrP at 0 hr of inhibitor treatment. **(C)** Total RNA was extracted from PC12 cells treated with MG132 as in (A), and murine and rat PrP mRNA levels were analyzed by Northern blotting (top panel). The EtBr-stained gel in the bottom panel demonstrates approximately equal loading of all lanes. Size markers are 18S and 28S rRNA. **(D)** PrP mRNA and EtBr signals from (C) were quantitated, and the ratio of PrP mRNA/rRNA at each time point was expressed relative to the ratio at 0 hr of inhibitor treatment.

FIGURE 6: An unglycosylated, signal peptide-bearing form of PrP accumulates after treatment of CHO cells with a proteasome inhibitor. Transiently transfected CHO cells expressing WT, PG14, or D177N PrPs were treated for 8 hrs with either ethanol vehicle (- lanes) or with PSI 1 (20 μM) (+ lanes). Cells were then lysed, and PrP analyzed by Western blotting using either 3F4 antibody or anti-signal peptide antibody (α-SP). The white and black arrowheads indicate the positions, respectively,

Downloaded from http://www.jbc.org/ by guest on March 24, 2020

of processed (signal peptide cleaved) and unprocessed (signal peptide-bearing) forms of unglycosylated PrP. These two species are not completely resolved for PG14 PrP, because of the higher M_r of this protein. The slightly faster migration of all bands in lane 9 compared to those in lane 10 is an artifact of gel smiling. Transiently transfected cells produce less doubly glycosylated PrP than stably transfected cells, accounting for the difference in the pattern of PrP bands between this figure and Fig. 4A.

FIGURE 7: The signal peptide-bearing form of PrP has a short metabolic half-life, and is stabilized in the presence of a proteasome inhibitor. (A, B) Transiently transfected CHO cells expressing WT PrP were pulse-labeled with [^{35}S]methionine for 20 min, and then chased in medium containing unlabeled methionine for 0, 0.5, 1, 2, 4, or 6 hrs. In one set of cultures (gels on the right), PSI-1 (20 μM) was present during a 30 min pre-incubation, as well as during the pulse and chase periods. In the other set of cultures (gels on the left), an equivalent amount of ethanol vehicle was present. At the end of the chase period, cells were lysed, and PrP was immunoprecipitated using either **(A)** 3F4 or **(B)** anti-SP antibodies, and analyzed by SDS-PAGE and autoradiography. The white and black arrowheads indicate the positions, respectively, of processed (signal peptide cleaved) and unprocessed (signal peptide-bearing) forms of unglycosylated PrP. **(C)** The amount of label in all PrP bands (unglycosylated + glycosylated) was calculated at each chase time as a percentage of the initial label, based on PhosphorImager analysis of the gels shown in (A). The results are representative of two independent experiments. **(D)** The amount of label in the signal peptide-bearing PrP band was calculated at each chase time as a percentage

Downloaded from http://www.jbc.org/ by guest on March 24, 2020

of the initial label, based on PhosphorImager analysis of the gels shown in (B). The results are representative of two independent experiments.

FIGURE 8: The signal peptide-bearing form of PrP that accumulates in the presence of proteasome inhibitor is present on the cytoplasmic side of the ER membrane, and is detergent-insoluble. (A) Transiently transfected BHK cells expressing WT PrP were treated for 16 hrs with either ethanol vehicle (lanes 1-3) or with PSI 1 (20 μM) (lanes 4-6). Postnuclear supernatants were then prepared, and were either left untreated (lanes 1 and 4), or were incubated with proteinase K in the absence (lanes 2 and 5) or presence (lanes 3 and 6) of Triton X-100 (Det). The arrow points to the PSI 1-induced form of PrP (lane 4) that is selectively digested with proteinase K in the absence of detergent (lane 5). **(B)** Transiently transfected CHO cells expressing WT PrP were treated for 16 hrs with either ethanol vehicle (lanes 1 and 2) or with PSI 1 (20 μM) (lanes 3 and 4). Cell lysates were first pre-cleared by centrifugation at 16,000 x g, and were subjected to centrifugation at 186,000 x g for 40 min. PrP in equivalent amounts of supernatants (lanes 1 and 3) and pellets (lanes 2 and 4) was then visualized by Western blotting. The arrow indicates the position of the PSI 1-induced form of PrP, which is detergent-insoluble (lane 4).

FIGURE 9: The signal peptide-bearing form of PrP that accumulates in the presence of proteasome inhibitor co-localizes with an ER marker. Stably transfected CHO cells expressing WT PrP were left untreated **(A-C)**, or were treated for 15 hr with 20 μM PSI **(D-F)**. Cells were then fixed and permeabilized, and stained with

Downloaded from http://www.jbc.org/ by guest on March 24, 2020

anti-SP and anti-PDI primary antibodies, followed by Alexa 488- and Alexa 594-conjugated secondary antibodies. Cells were viewed with green excitation/emission settings to detect signal peptide-bearing PrP **(A, D)**, and with red excitation/emission settings to detect PDI **(B, E)**. Merged red and green images are shown in **C** and **F**. All cells in F show colocalization of PrP and PDI, although several cells do not appear yellow because they contain lower levels of PDI, so the red and green signals are not matched in intensity. The scale bar in F is 50 μm (applicable to all panels).

FIGURE 10: Proteasome inhibitors do not cause accumulation of PrP in cerebellar granule neurons. Cerebellar granule neurons from transgenic mice expressing either WT PrP **(A)** or PG14 PrP **(B)** were treated with MG132 (5 μM) for 0, 1, 2, 4, 8, or 24 hrs. Cells were then lysed, and analyzed by Western blotting using either 3F4 antibody (upper panel) or anti-ubiquitin antibody (lower panel). Each pair of lanes represents duplicate cultures. **(C)** The same lysates used in panels A and B were Western blotted using anti-SP antibody (lanes 1-12). Lysates of transfected PC12 cells expressing WT or PG14 PrP that had been treated for 24 hrs with MG132 (10 μM) were run in lane 13 to serve as size markers for the respective signal peptide-containing forms.

Downloaded from http://www.jbc.org/ by guest on March 24, 2020

FIGURE 1

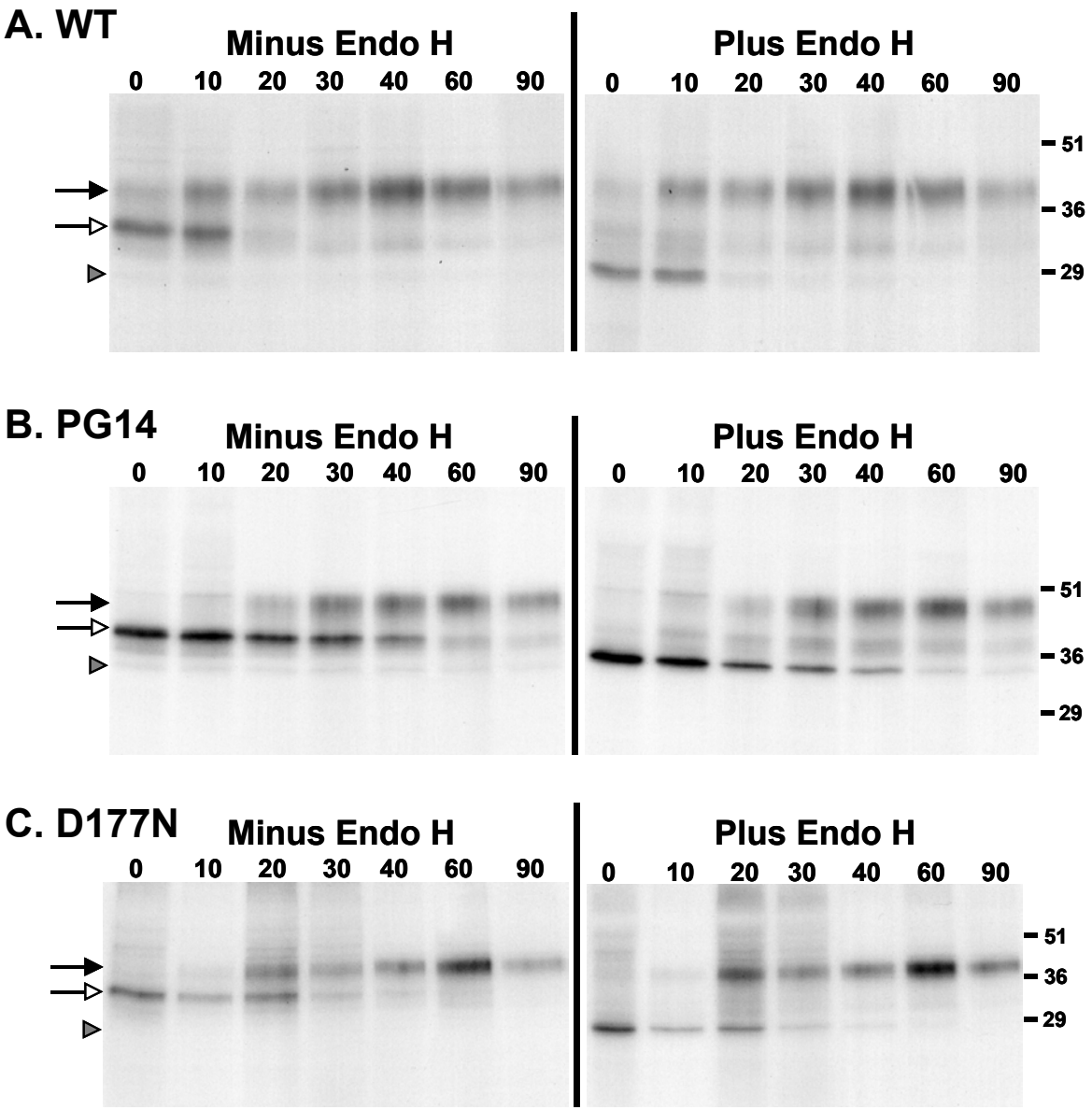
A. WT
Minus Endo H
Plus Endo H
0 10 20 30 40 60 90
0 10 20 30 40 60 90
51
36
29
B. PG14
Minus Endo H
Plus Endo H
0 10 20 30 40 60 90
0 10 20 30 40 60 90
51
36
29
C. D177N
Minus Endo H
Plus Endo H
0 10 20 30 40 60 90
0 10 20 30 40 60 90
51
36
29

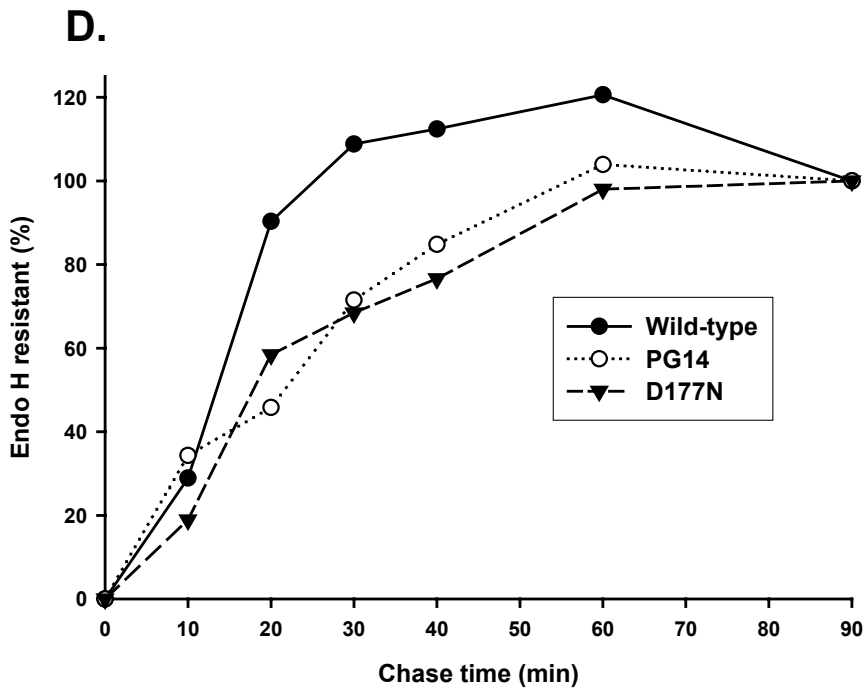
D.
Endo H resistant (%)
0
20
40
60
80
100
120
0 10 20 30 40 50 60 70 80 90
Chase time (min)
Wild-type
PG14
D177N

FIGURE 2

A. WT

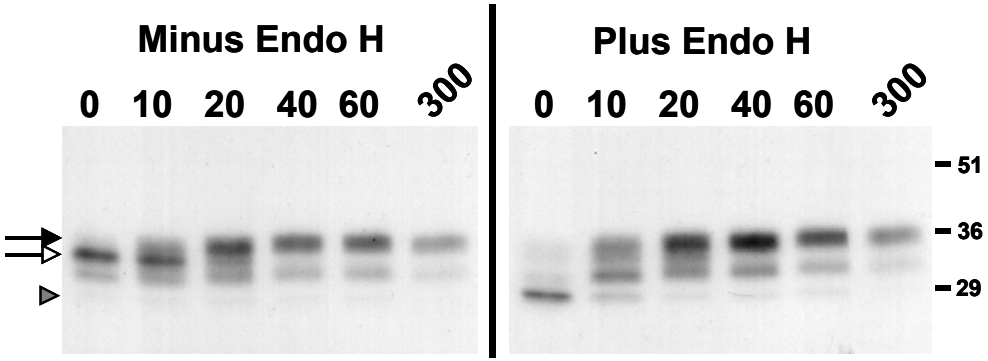

B. PG14

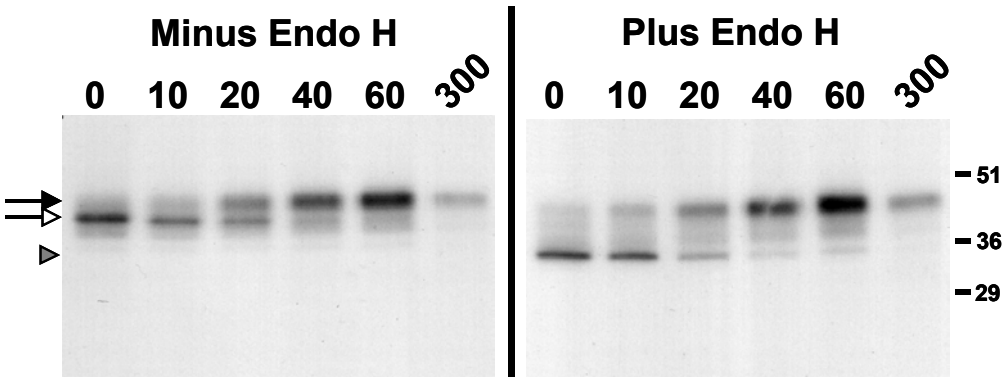

C.

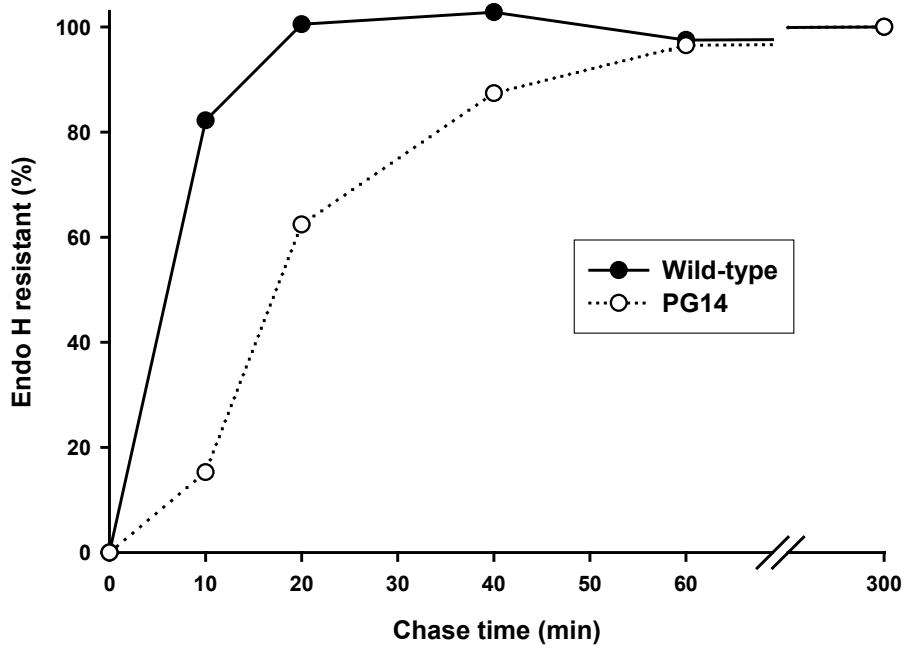

FIGURE 3

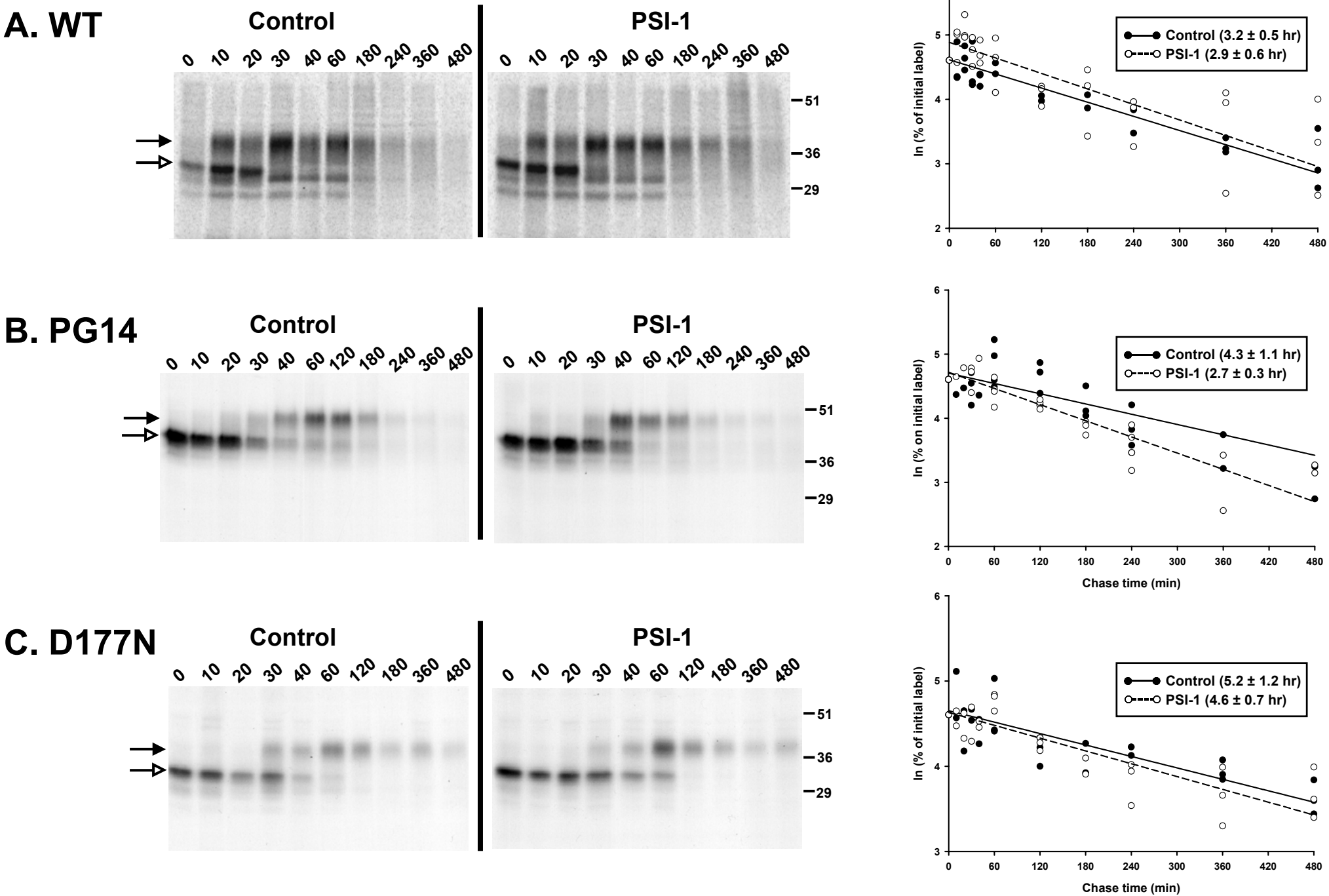
A. WT
Control
PSI-1
0 10 20 30 40 60 180 240 360 480
51
36
29
Control (3.2 ± 0.5 hr)
PSI-1 (2.9 ± 0.6 hr)
ln (% of initial label)
B. PG14
Control
PSI-1
0 10 20 30 40 60 120 180 240 360 480
51
36
29
Control (4.3 ± 1.1 hr)
PSI-1 (2.7 ± 0.3 hr)
ln (% on initial label)
Chase time (min)
C. D177N
Control
PSI-1
0 10 20 30 40 60 120 180 360 480
51
36
29
Control (5.2 ± 1.2 hr)
PSI-1 (4.6 ± 0.7 hr)
ln (% of initial label)
Chase time (min)

FIGURE 4

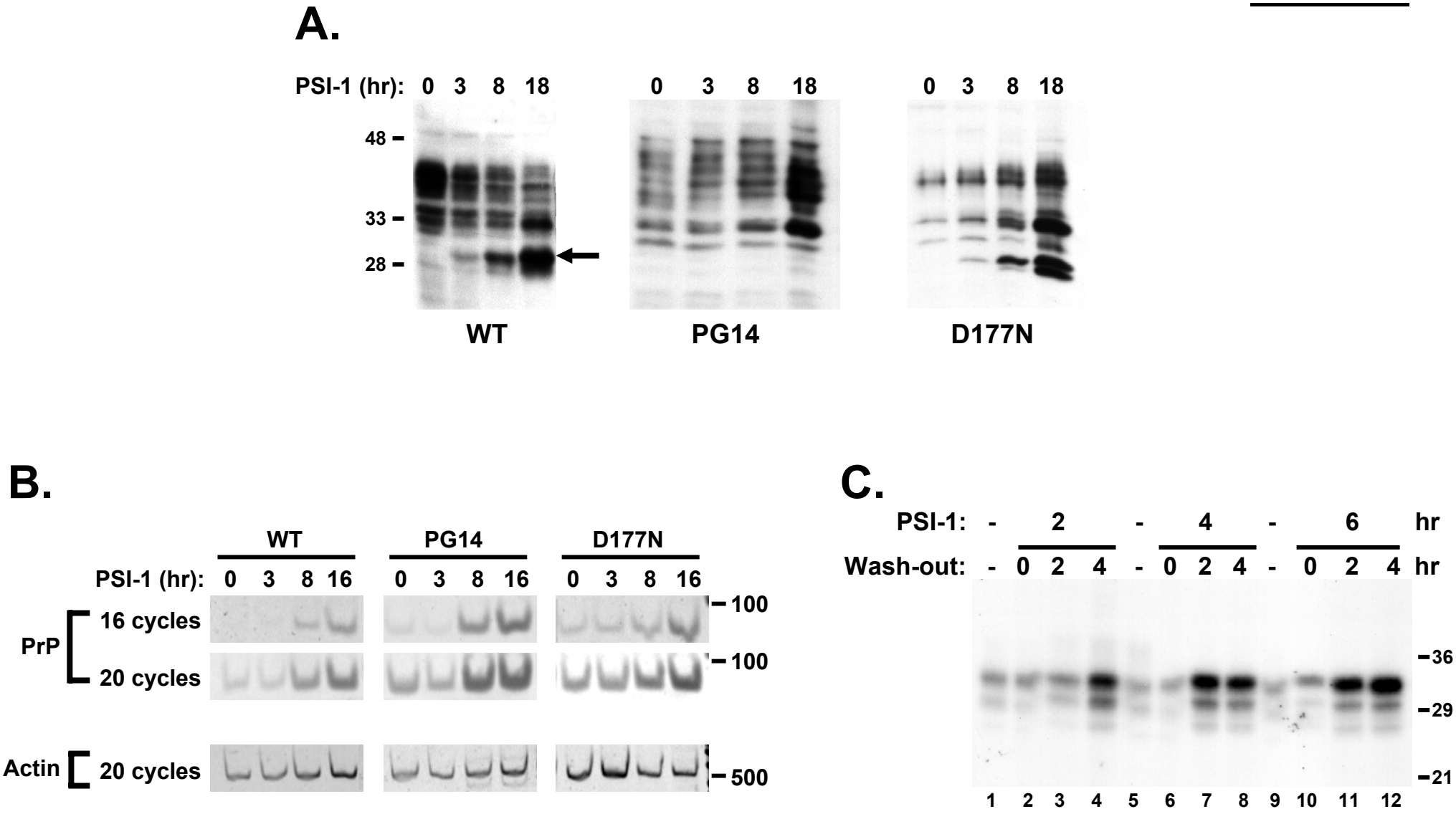
A.
PSI-1 (hr): 0 3 8 18
0 3 8 18
0 3 8 18
48
33
28
WT
PG14
D177N
B.
WT
PG14
D177N
PSI-1 (hr): 0 3 8 16
0 3 8 16
0 3 8 16
PrP
16 cycles
20 cycles
Actin
20 cycles
100
100
500
C.
PSI-1: - 2 - 4 - 6 hr
Wash-out: - 0 2 4 - 0 2 4 - 0 2 4 hr
36
29
21
1 2 3 4 5 6 7 8 9 10 11 12

FIGURE 5

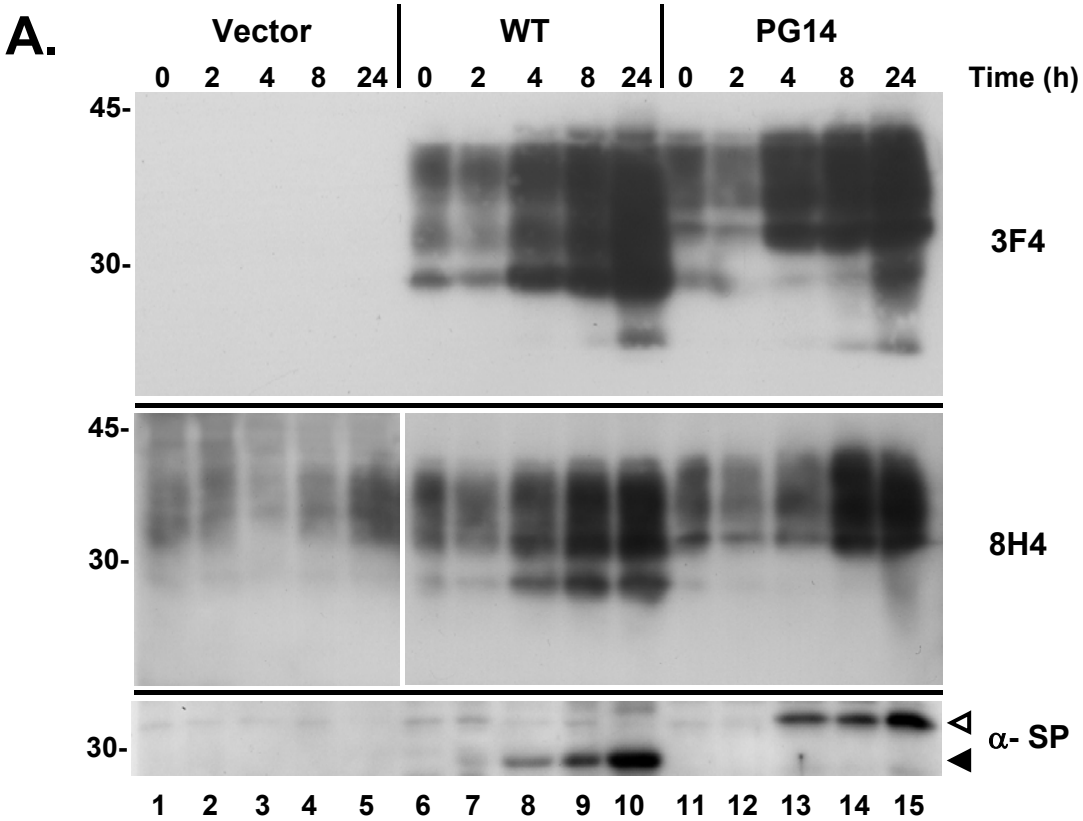
A.
Vector
WT
PG14
0 2 4 8 24 0 2 4 8 24 0 2 4 8 24
Time (h)
45-
30-
3F4
45-
30-
8H4
30-
α- SP
1 2 3 4 5 6 7 8 9 10 11 12 13 14 15

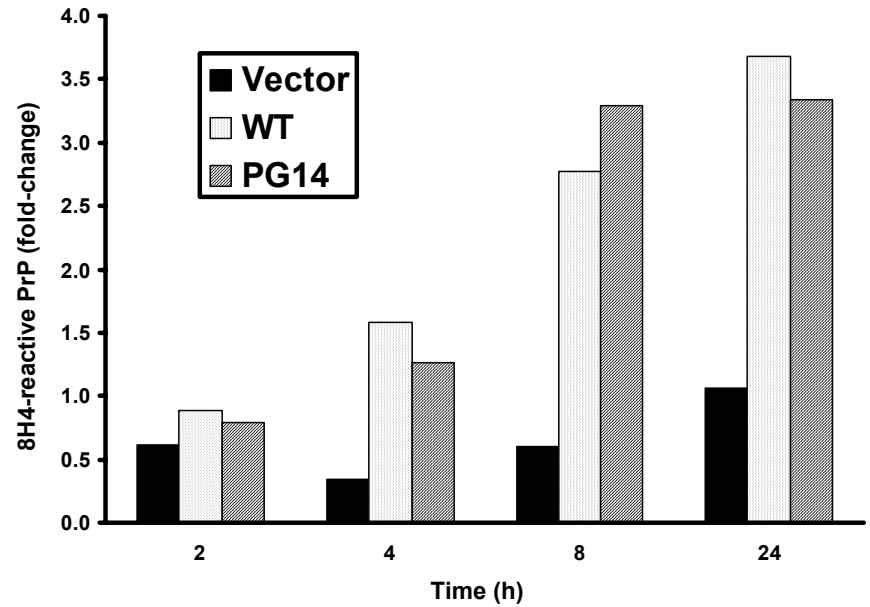
B.
8H4-reactive PrP (fold-change)
Vector
WT
PG14
4.0
3.5
3.0
2.5
2.0
1.5
1.0
0.5
0.0
2
4
8
24
Time (h)

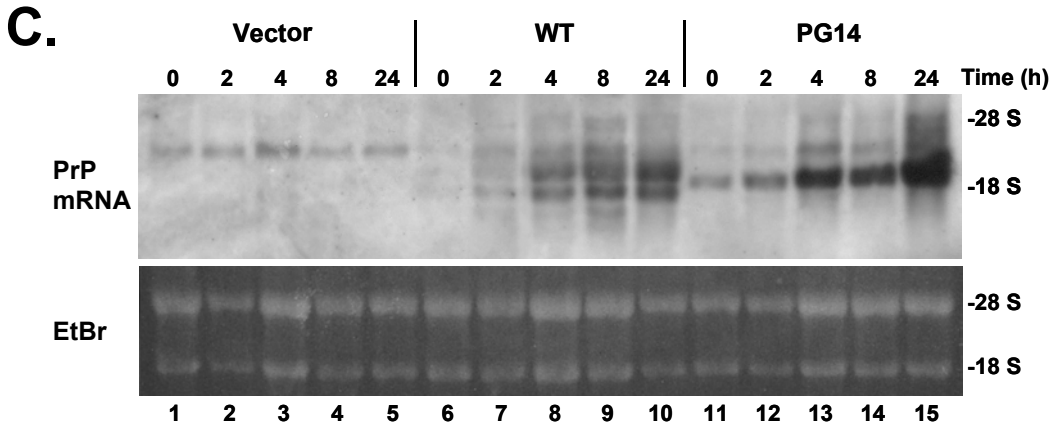
C.
Vector
WT
PG14
0 2 4 8 24 0 2 4 8 24 0 2 4 8 24
Time (h)
PrP mRNA
-28 S
-18 S
EtBr
-28 S
-18 S
1 2 3 4 5 6 7 8 9 10 11 12 13 14 15

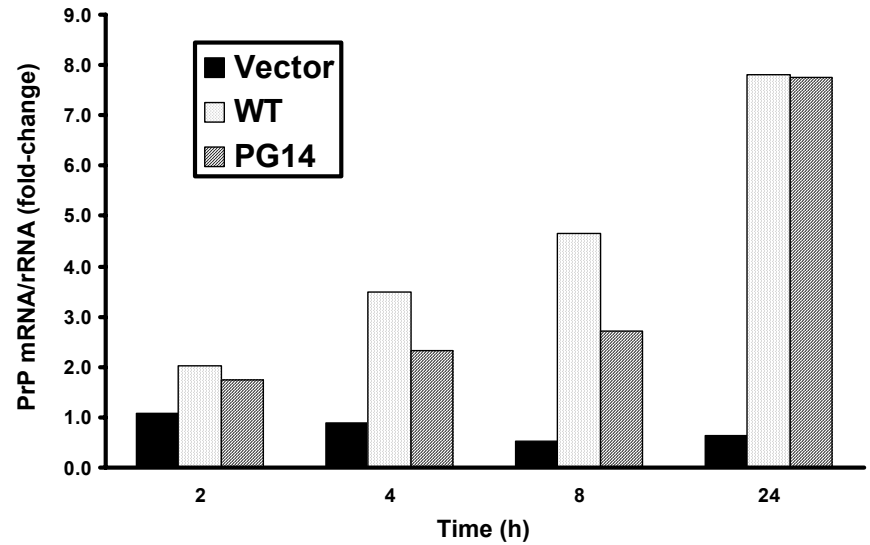
D.
PrP mRNA/rRNA (fold-change)
Vector
WT
PG14
9.0
8.0
7.0
6.0
5.0
4.0
3.0
2.0
1.0
0.0
2
4
8
24
Time (h)

FIGURE 6

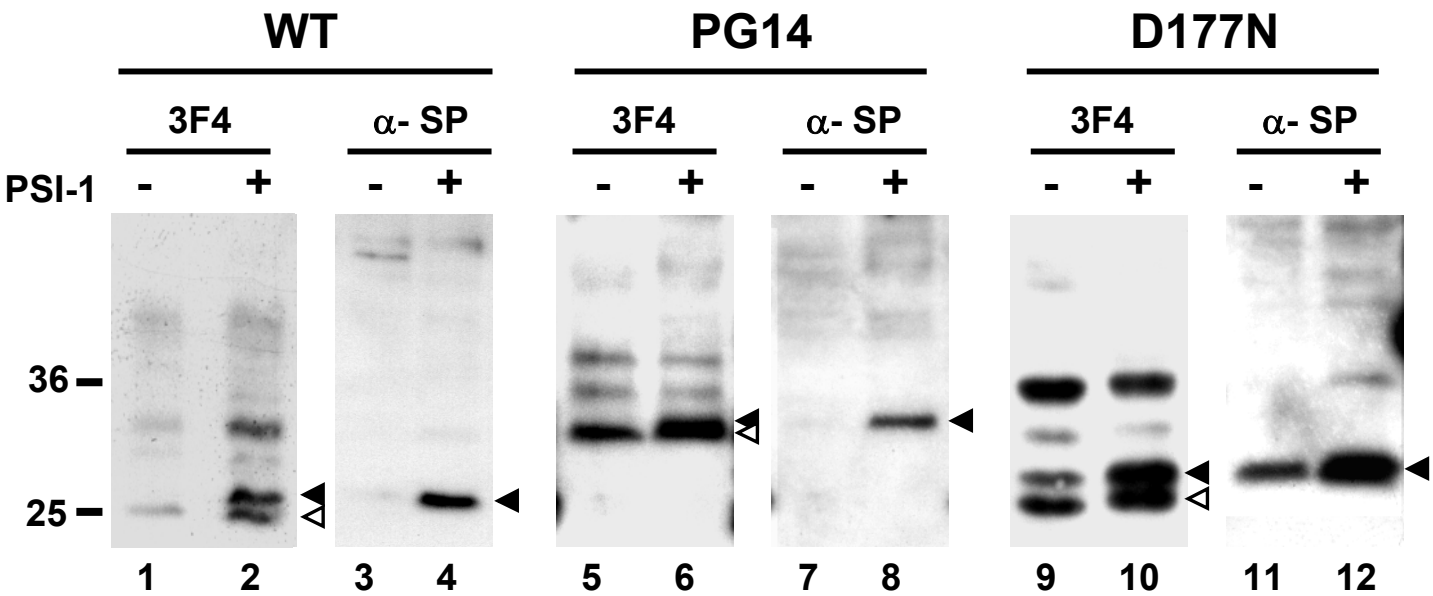
WT
PG14
D177N
3F4
α- SP
3F4
α- SP
3F4
α- SP
PSI-1
- + - + - + - + - + - +
36
25
1 2 3 4 5 6 7 8 9 10 11 12

FIGURE 7

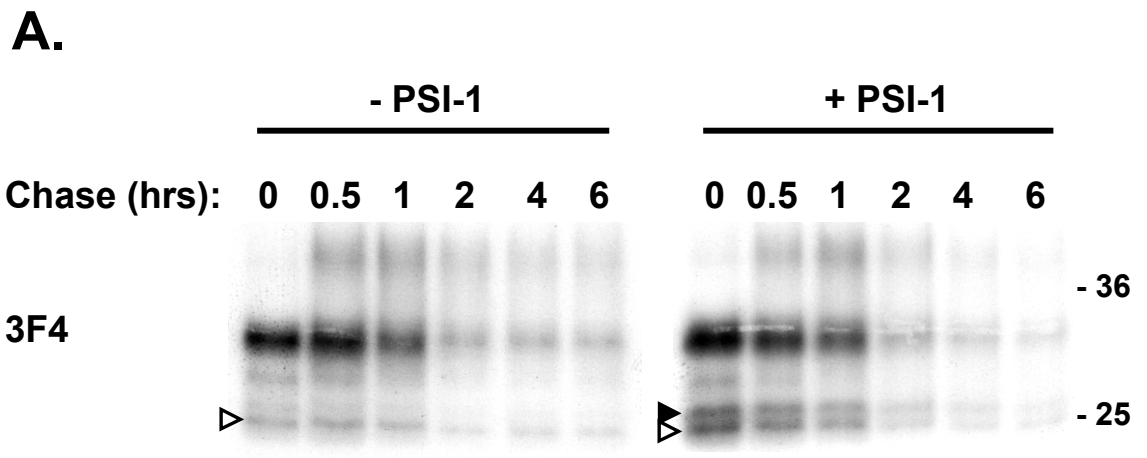
A.
- PSI-1
+ PSI-1
Chase (hrs): 0 0.5 1 2 4 6 0 0.5 1 2 4 6
3F4
- 36
- 25

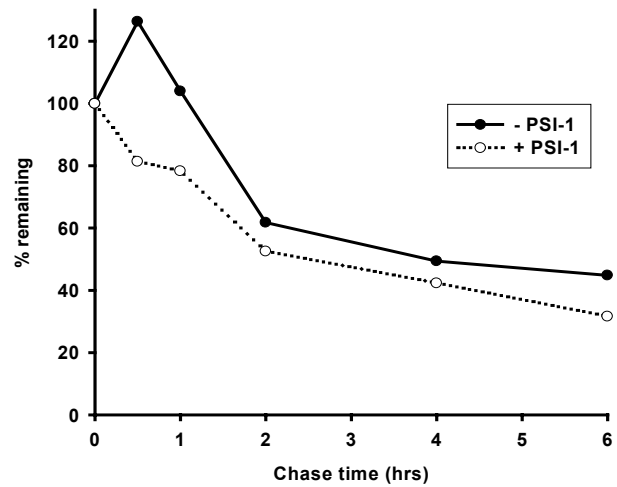
C.
% remaining
Chase time (hrs)
- PSI-1
+ PSI-1

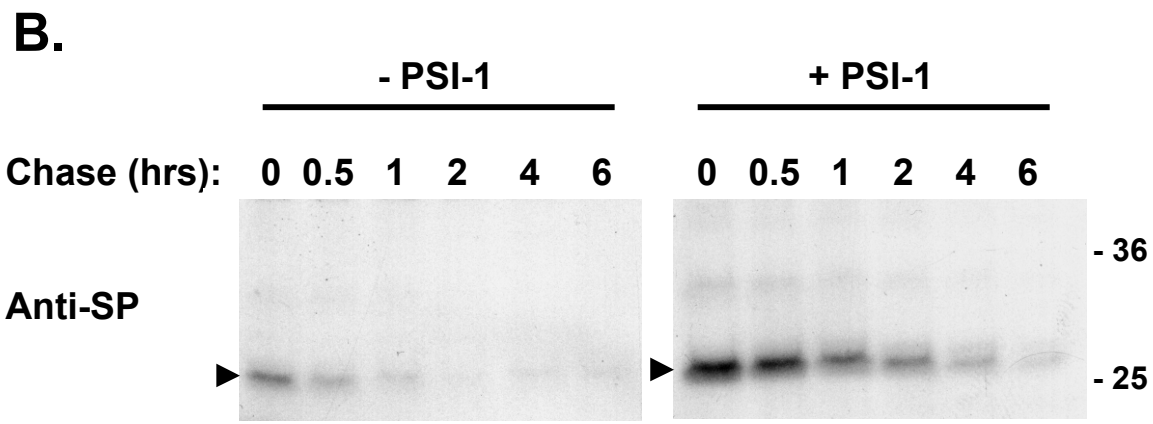
B.
- PSI-1
+ PSI-1
Chase (hrs): 0 0.5 1 2 4 6 0 0.5 1 2 4 6
Anti-SP
- 36
- 25

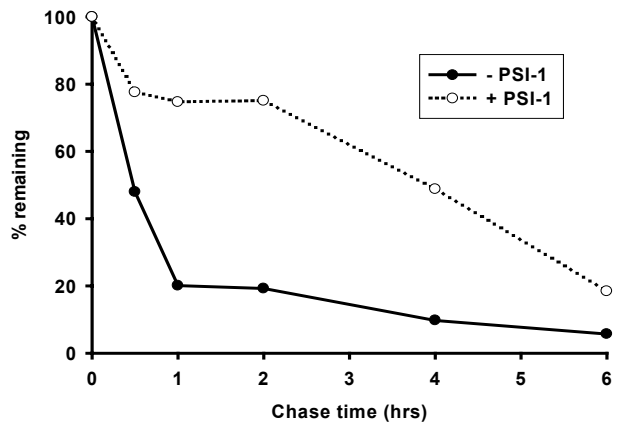
D.
% remaining
Chase time (hrs)
- PSI-1
+ PSI-1

FIGURE 8

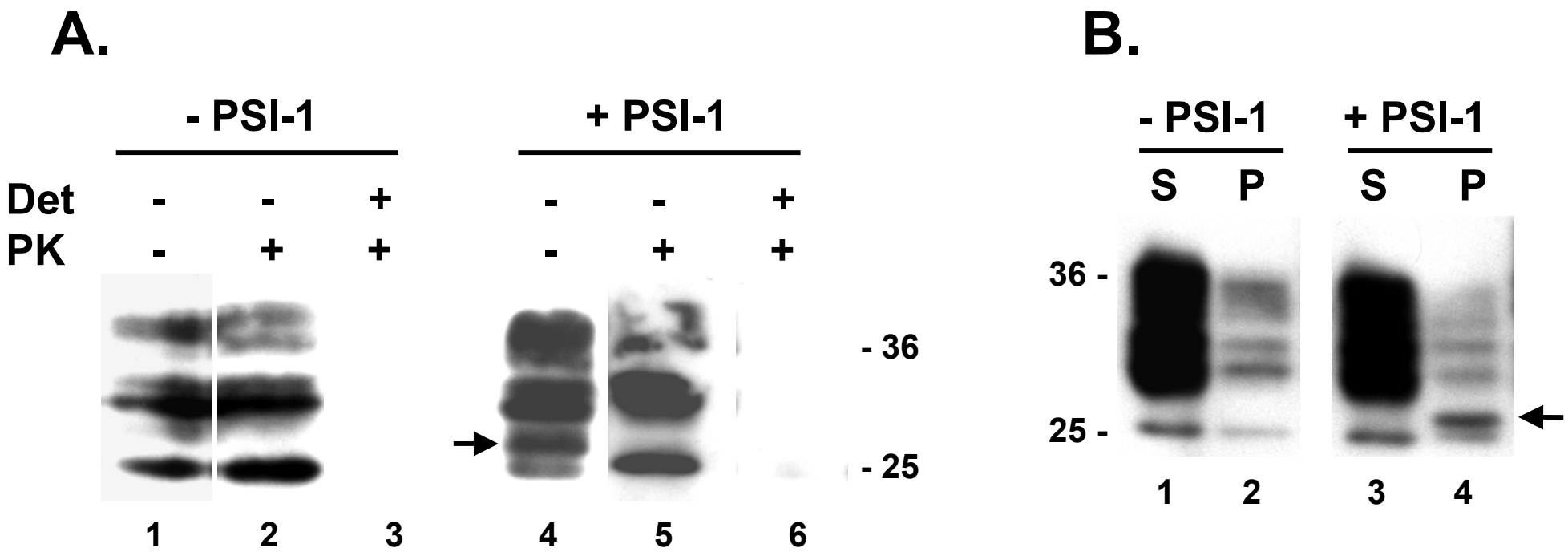

FIGURE 9

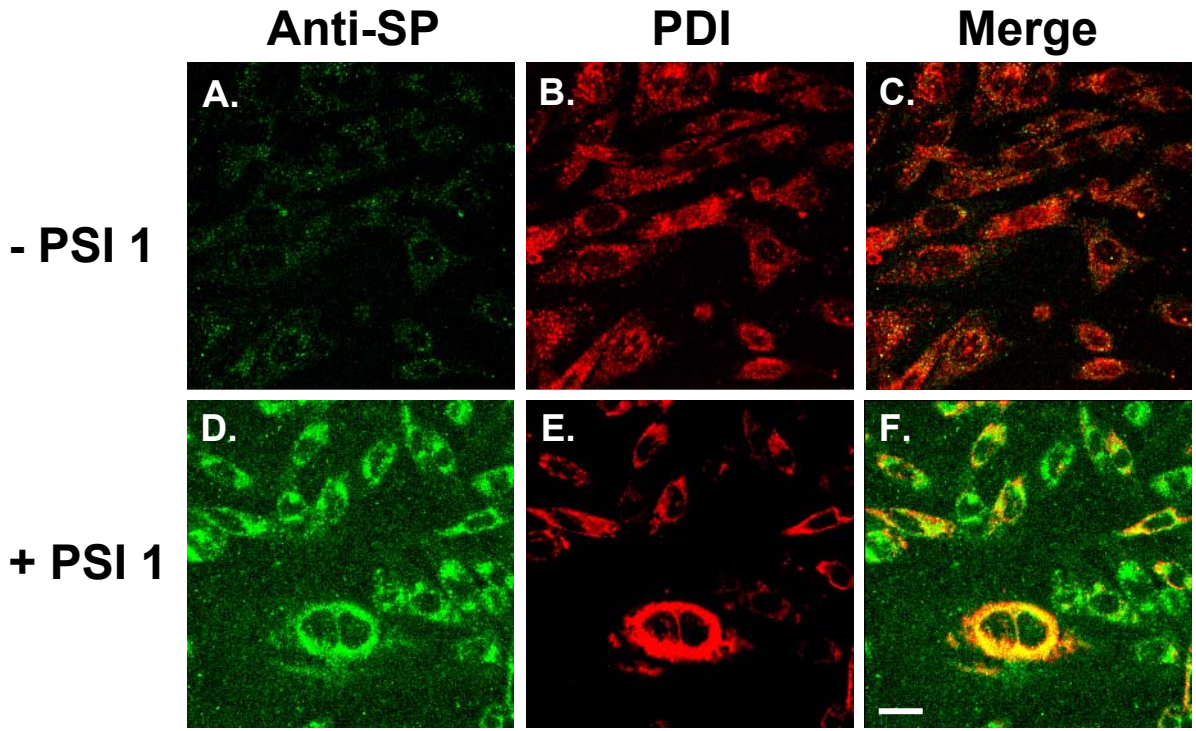

FIGURE 10

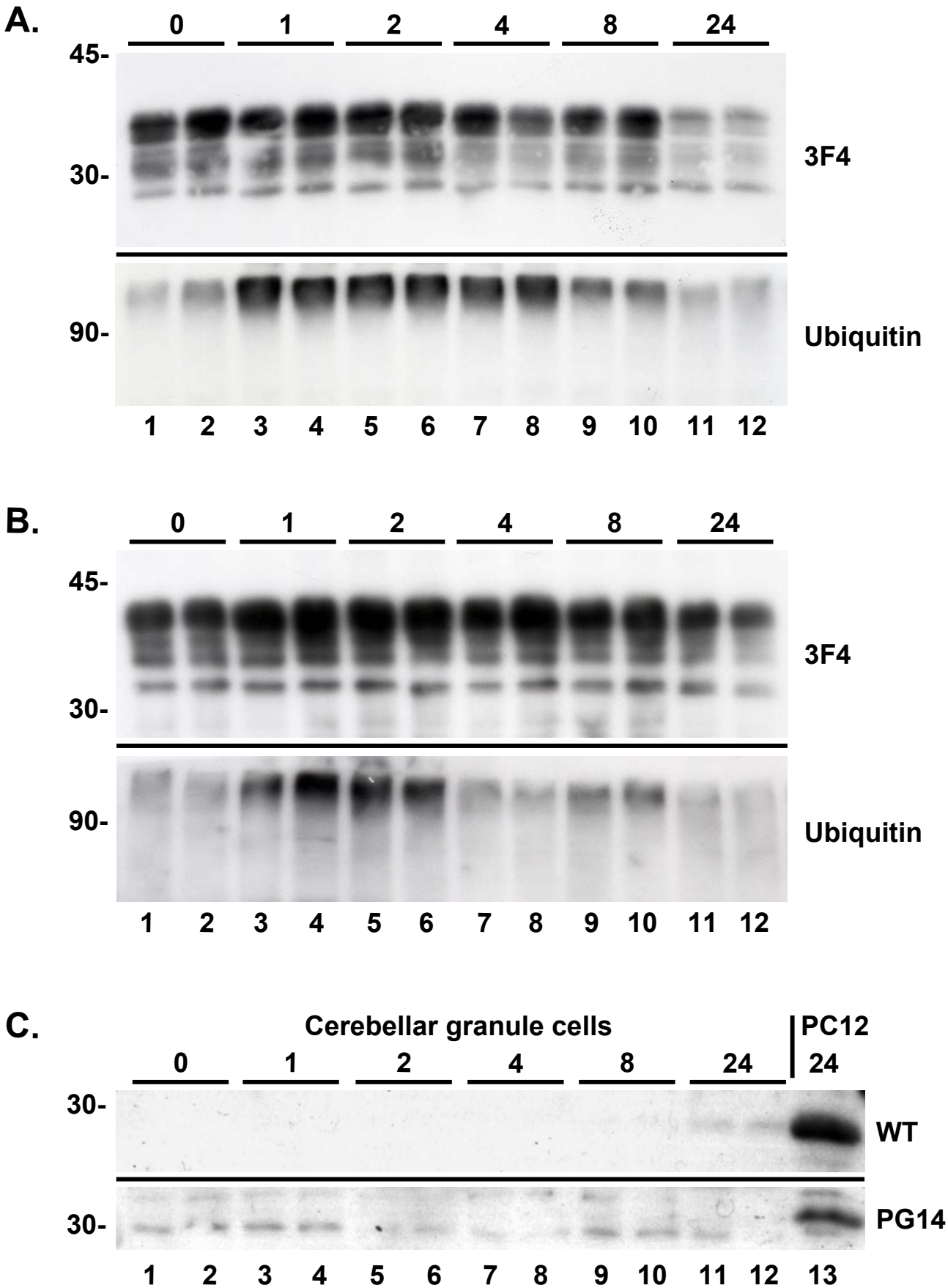
A.
0
1
2
4
8
24
45-
30-
3F4
90-
Ubiquitin
1 2 3 4 5 6 7 8 9 10 11 12
B.
0
1
2
4
8
24
45-
30-
3F4
90-
Ubiquitin
1 2 3 4 5 6 7 8 9 10 11 12
C.
Cerebellar granule cells
PC12
0
1
2
4
8
24
24
30-
WT
30-
PG14
1 2 3 4 5 6 7 8 9 10 11 12 13

Mutant PrP is delayed in its exit from the endoplasmic reticulum, but neither wild-type nor mutant PrP undergoes retrotranslocation prior to proteasomal degradation ^

Bettina Drisaldi, Richard S. Stewart, Cheryl Adles, Leanne R. Stewart, Elena Quaglio, Emiliano Biasini, Luana Fioriti, Roberto Chiesa and David A. Harris

J. Biol. Chem. published online March 26, 2003

Access the most updated version of this article at doi: 10.1074/jbc.M213247200

Alerts:
- When this article is cited
- When a correction for this article is posted

Click here to choose from all of JBC's e-mail alerts

Downloaded from http://www.jbc.org/ by guest on March 24, 2020